Contents

Chapter 2

Metals

2.1 Introduction

Metals are characterized by a finite electronic density of states $f(\varepsilon_{\rm F})$ at the Fermi level at zero temperature. This entails a number of salient features, such as thermodynamic, electrodynamic, and transport properties.

2.2 $T = 0$ and the Fermi Surface

2.2.1 Definition of the Fermi surface

The Pauli principle says that each fermionic energy state can accommodate either zero or one electrons[1]. At zero temperature, the ground state of a noninteracting Fermi gas is obtained by filling up all the distinct eigenstates in order of energy, starting from the bottom of the spectrum, until all the fermions are used up. The energy of the last level to be filled is called the *Fermi energy*, and is written $\varepsilon_{\rm F}$. The energy distribution function at $T = 0$ is thus $n(\varepsilon) = \Theta(\varepsilon_{\rm F} - \varepsilon)$, which says that all single particle energy states up to $\varepsilon = \mu$ are filled, and all energy states above $\varepsilon = \mu$ are empty. As we shall see in the next section, the Fermi energy is the zero temperature value of the chemical potential: $\varepsilon_{\rm F} = \mu(T = 0)$. If the single particle dispersion $\varepsilon(\boldsymbol{k})$ depends only on the wavevector $\boldsymbol{k}$, then the locus of points in $\boldsymbol{k}$-space for which $\varepsilon(\boldsymbol{k}) = \varepsilon_{\rm F}$ is called the *Fermi surface*. For isotropic systems, $\varepsilon(\boldsymbol{k}) = \varepsilon(k)$ is a function only of the magnitude $k = |\boldsymbol{k}|$, and the Fermi surface is a sphere in $d = 3$ or a circle in $d = 2$. The radius of this circle is the *Fermi wavevector*, $k_{\rm F}$. When there is internal (*e.g.* spin) degree of freedom, there is a Fermi surface and Fermi wavevector (for isotropic systems) for each polarization state of the internal degree of freedom.

Let's compute the Fermi wavevector $k_{\rm F}$ and Fermi energy $\varepsilon_{\rm F}$ for the IFG with a ballistic dispersion $\varepsilon(\boldsymbol{k}) = \hbar^2\boldsymbol{k}^2/2m$. We allow for a common degeneracy g for each of the $\boldsymbol{k}$ states, *e.g.*, due to spin, for

[1] We consider two degenerate energy states with different spin polarizations $\uparrow$ and $\downarrow$ to be distinct quantum states.

which $\mathsf{g} = 2S + 1$, with $S = \frac{1}{2}$ for electrons. The number density is

$$n = \mathsf{g}\int d^dk\,\Theta(k_{\rm F} - k) = \frac{\mathsf{g}\,\Omega_d}{(2\pi)^d}\cdot\frac{k_{\rm F}^d}{d} = \begin{cases} \mathsf{g}\,k_{\rm F}/\pi & (d=1) \\ \mathsf{g}\,k_{\rm F}^2/4\pi & (d=2) \\ \mathsf{g}\,k_{\rm F}^3/6\pi^2 & (d=3) \end{cases}, \tag{2.1}$$

where $\Omega_d = 2\pi^{d/2}/\Gamma(d/2)$ is the area of the unit sphere in d space dimensions ($\Omega_1 = 2$, $\Omega_2 = 2\pi$, $\Omega_3 = 4\pi$, *etc.*). Note that the form of $n(k_{\rm F})$ is independent of the dispersion relation, so long as it remains isotropic. Inverting the above expressions, we obtain $k_{\rm F}(n)$:

$$k_{\rm F} = 2\pi\left(\frac{d\,n}{\mathsf{g}\,\Omega_d}\right)^{1/d} = \begin{cases} \pi n/\mathsf{g} & (d=1) \\ (4\pi n/\mathsf{g})^{1/2} & (d=2) \\ (6\pi^2 n/\mathsf{g})^{1/3} & (d=3) \end{cases}. \tag{2.2}$$

The Fermi energy in each case, for ballistic dispersion, is therefore

$$\varepsilon_{\rm F} = \frac{\hbar^2 k_{\rm F}^2}{2m} = \frac{2\pi^2\hbar^2}{m}\left(\frac{d\,n}{\mathsf{g}\,\Omega_d}\right)^{2/d} = \begin{cases} \frac{\pi^2\hbar^2 n^2}{2\mathsf{g}^2 m} & (d=1) \\ \frac{2\pi\hbar^2\,n}{\mathsf{g}\,m} & (d=2) \\ \frac{\hbar^2}{2m}\left(\frac{6\pi^2 n}{\mathsf{g}}\right)^{2/3} & (d=3) \end{cases}. \tag{2.3}$$

Another useful result for the ballistic dispersion, which follows from the above, is that the density of states at the Fermi level is given by

$$g(\varepsilon_{\rm F}) = \frac{\mathsf{g}\,\Omega_d}{(2\pi)^d}\cdot\frac{m k_{\rm F}^{d-2}}{\hbar^2} = \frac{d}{2}\cdot\frac{n}{\varepsilon_{\rm F}} \quad . \tag{2.4}$$

For the electron gas, we have $\mathsf{g} = 2$. In a metal, one typically has $k_{\rm F} \sim 0.5\,\text{Å}^{-1}$ to $2\,\text{Å}^{-1}$, and $\varepsilon_{\rm F} \sim 1\,\text{eV} - 10\,\text{eV}$. Due to the effects of the crystalline lattice, electrons in a solid behave as if they had an *effective mass* m^* which is typically on the order of the electron mass but very often about an order of magnitude smaller, particularly in semiconductors.

In solids, the dispersions $\varepsilon(\boldsymbol{k})$ are in general anisotropic, and give rise to non-spherical Fermi surfaces. The simplest example is that of a two-dimensional tight-binding model of electrons hopping on a square lattice, as may be appropriate in certain layered materials. The dispersion relation is then

$$\varepsilon(k_x, k_y) = -2t\,\cos(k_x a) - 2t\,\cos(k_y a)\,, \tag{2.5}$$

where k_x and k_y are confined to the interval $\left[-\frac{\pi}{a}, \frac{\pi}{a}\right]$. The quantity t has dimensions of energy and is known as the *hopping integral*. The Fermi surface is the set of points (k_x, k_y) which satisfies $\varepsilon(k_x, k_y) = \varepsilon_{\rm F}$.

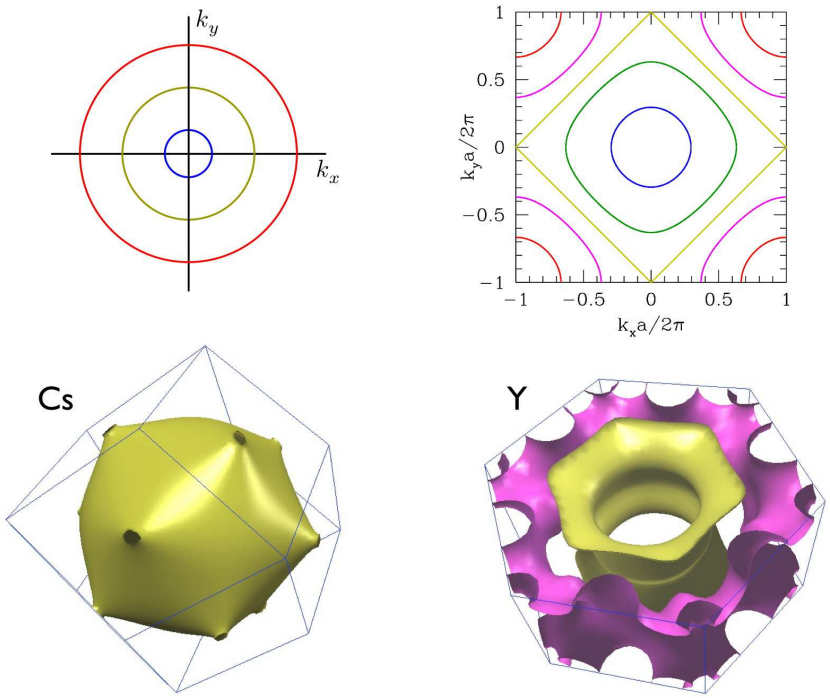

Figure 2.1: Fermi surfaces for two and three-dimensional structures. Upper left: free particles in two dimensions. Upper right: 'tight binding' electrons on a square lattice. Lower left: Fermi surface for cesium, which is predominantly composed of electrons in the $6s$ orbital shell. Lower right: the Fermi surface of yttrium has two parts. One part (yellow) is predominantly due to $5s$ electrons, while the other (pink) is due to $4d$ electrons. (Source: www.phys.ufl.edu/fermisurface/)

When $\varepsilon_{\rm F}$ achieves its minimum value of $\varepsilon_{\rm F}^{\rm min} = -4t$, the Fermi surface collapses to a point at $(k_x, k_y) = (0, 0)$. For energies just above this minimum value, we can expand the dispersion in a power series, writing

$$\varepsilon(k_x, k_y) = -4t + ta^2 \left(k_x^2 + k_y^2\right) - \tfrac{1}{12}\, ta^4 \left(k_x^4 + k_y^4\right) + \dots \ . \tag{2.6}$$

If we only work to quadratic order in k_x and k_y, the dispersion is isotropic, and the Fermi surface is a circle, with $k_{\rm F}^2 = (\varepsilon_{\rm F} + 4t)/ta^2$. As the energy increases further, the continuous $\mathrm{O}(2)$ rotational invariance is broken down to the discrete group of rotations of the square, C_{4v}. The Fermi surfaces distort and eventually, at $\varepsilon_{\rm F} = 0$, the Fermi surface is itself a square. As $\varepsilon_{\rm F}$ increases further, the square turns back into a circle, but centered about the point $\left(\frac{\pi}{a}, \frac{\pi}{a}\right)$. Note that everything is periodic in k_x and k_y modulo $\frac{2\pi}{a}$. The Fermi surfaces for this model are depicted in the upper right panel of fig. 2.1.

Fermi surfaces in three dimensions can be very interesting indeed, and of great importance in understanding the electronic properties of solids. Two examples are shown in the bottom panels of fig. 2.1. The electronic configuration of cesium (Cs) is $[\mathrm{Xe}]\, 6s^1$. The $6s$ electrons 'hop' from site to site on a body centered cubic (BCC) lattice, a generalization of the simple two-dimensional square lattice hopping model discussed above. The elementary unit cell in $\boldsymbol{k}$ space, known as the *first Brillouin zone*, turns out to be a dodecahedron. In yttrium, the electronic structure is $[\mathrm{Kr}]\, 5s^2\, 4d^1$, and there are two electronic energy bands at the Fermi level, meaning two Fermi surfaces. Yttrium forms a hexagonal close packed (HCP)

crystal structure, and its first Brillouin zone is shaped like a hexagonal pillbox.

2.2.2 Fermi surface vs. Brillouin zone

The construction of the first Brillouin zone proceeds as follows. Draw the bisecting planes ($d = 3$) or lines ($d = 2$) for each of the reciprocal lattice vectors $\boldsymbol{G} = \sum_{\mu=1}^{d} n_\mu \boldsymbol{b}_\mu$. The region bounded by these bisectors which contains the origin is the first Brillouin zone. The regions for which a minimum of one bisector is crossed in order to get to the first zone defines the second zone. Points for which a minimum of $(j-1)$ bisectors must be crossed to arrive in the first zone comprise the $j^{\rm th}$ zone. For the square lattice, this scheme is depicted in Fig. 2.2. By shifting all the various fragments of the $j^{\rm th}$ zone by reciprocal lattice vectors, one can completely cover the first zone, with no overlapping areas. Thus, the volume of each of the zones is always $\hat{v}_0$.

Suppose there are Z electrons per unit cell. The Fermi wavevector $k_{\rm F}$ is determined by $k_{\rm F} = (2\pi n)^{1/2}$ with $na^2 = Z$. The side length of the Brillouin zone is $b = 2\pi/a$. Thus, the ratio of the diameter of the free electron Fermi circle to the elementary RLV is

$$r \equiv \frac{2k_{\rm F}}{b} = \sqrt{\frac{2Z}{\pi}} \quad . \tag{2.7}$$

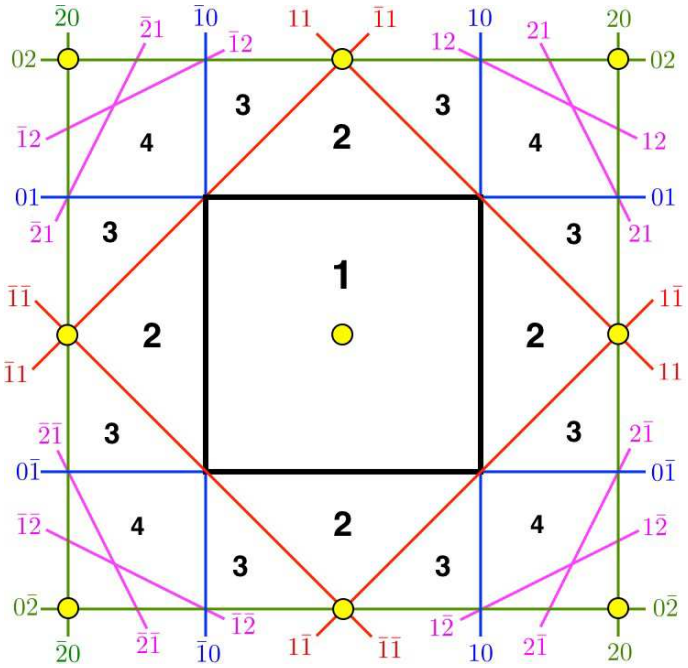

Figure 2.2: Extended zones and their folding for the square lattice. Reciprocal lattice points are shown as yellow dots. The central square, defined by the thick black line, is the first Brillouin zone. The colored lines denote bisectors of reciprocal lattice vectors $\boldsymbol{G} = n_1\boldsymbol{b}_1 + n_2\boldsymbol{b}_2$ and are labeled by n_1 and n_2. In general, a minimum of $j-1$ such bisectors must be crossed in going from the $j^{\rm th}$ Brillouin zone to the first Brillouin zone., with j labeled in black. (Not all of the fourth zone is labeled.)

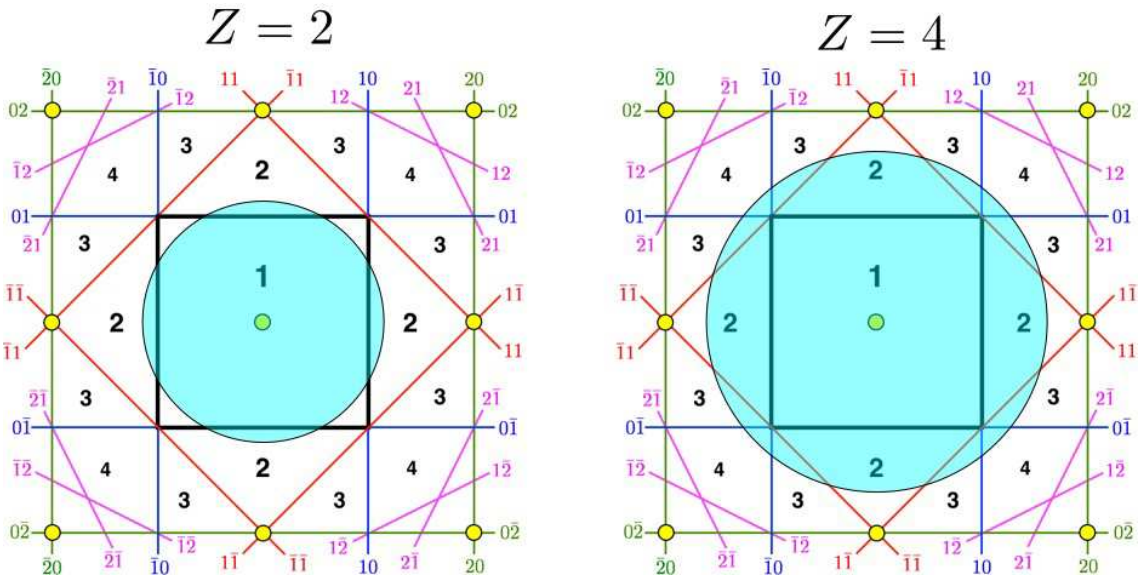

Figure 2.3: Brillouin zones and free electron Fermi seas (in blue) for the square lattice. Left: $Z = 2$ electrons per cell. The Fermi surface has area $\hat{v}_0$, and the free electron Fermi sea extends into the second zone. Right: $Z = 4$ electrons per cell. The Fermi surface has area $2\hat{v}_0$. and the free electron Fermi sea completely covers the first zone, and extends into portions of the second, third, and fourth zones.

If $r < 1$, the Fermi circle lies entirely within the first Brillouin zone $\widehat{\Omega}$. This is the case for $Z = 1$, when $r = 0.798$, but for $Z = 2$ the area of the Fermi circle is precisely the Brillouin zone area, and $r = (4/\pi)^{1/2} = 1.128$, so the Fermi circle spills over into the second zone. The situation is depicted in the left panel of Fig. 2.3. Since $r < \sqrt{2}$, it does not cross any of the red lines in the left panel, *i.e.* the Fermi circle is confined to the first and second zones. The effect of a weak crystalline potential, as we have seen, is to introduce energy gaps along the Brillouin zone boundaries. If the crystalline potential is strong enough, it can pull all of the states from the second zone into the first zone, completely filling it , thereby resulting in a band insulator.

When $Z = 3$, find $r = 1.382 < \sqrt{2}$, so again the Fermi surface lies only within the first and second zones. For $Z = 4$, $r = 1.596 > \sqrt{2}$, and as we see in the right panel of the figure, the Fermi sea completely encloses the first zone, and spills over into zones two, three, and four.

What happens in $d = 3$ dimensions? Fig. 2.4 shows some examples. Sodium (Na) is monovalent, and the volume of its free electron Fermi sphere is half that of the Brillouin zone and fits entirely within $\widehat{\Omega}$. The crystal structure is bcc and the first Brillouin zone has the shape of a rhombic dodecahedron. Copper (Cu) is also monovalent, but the crystalline potential is stronger and leads to the eight Fermi surface 'necks' shown in the figure. The crystal structure is fcc, and the Brillouin zone has the shape of a truncated octahedron. The necks straddle the eight hexagonal faces of the first zone. Calcium (Ca) is divalent, hence the free electron Fermi sphere has exactly the same volume as that of the first Brillouin zone. Thus, this sphere must cut across the Brillouin zone boundaries, resulting in two bands, the Fermi surface in the first of which is depicted in the figure. The lattice potential pulls most but not all of the states in the second zone into the first zone.

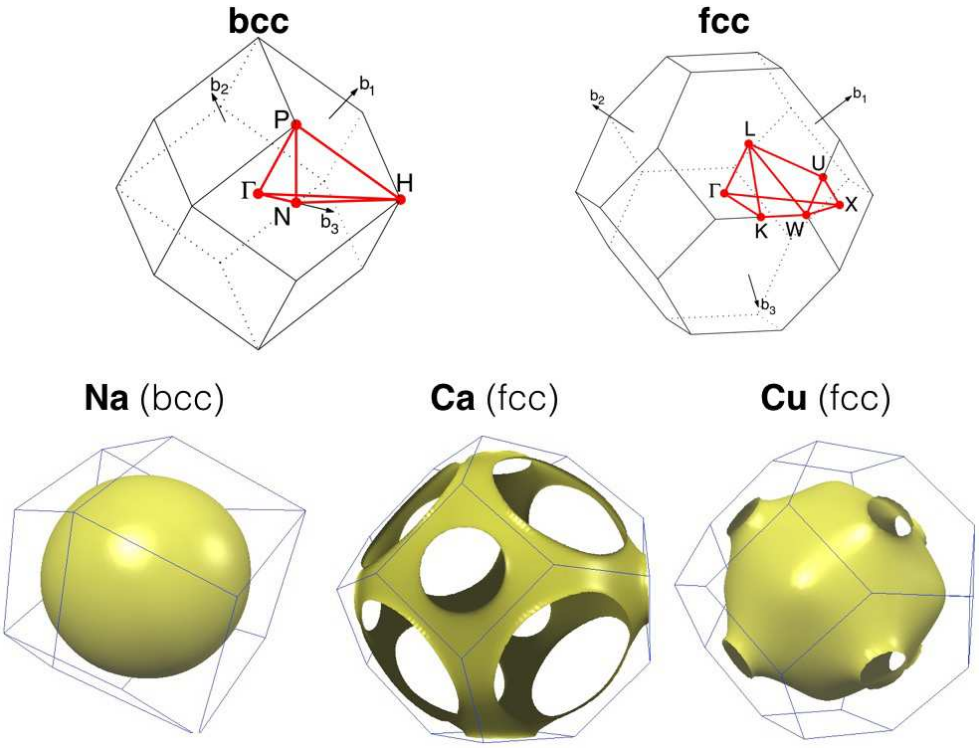

Figure 2.4: Top: First Brillouin zones for bcc (left) and fcc (right) lattice solids. Bottom: Fermi surfaces for Na (left), Ca (center), and Cu (right). (Source: www.phys.ufl.edu/fermisurface/)

2.2.3 Spin-split Fermi surfaces

Consider an electron gas in an external magnetic field H. The single particle Hamiltonian is then

$$\hat{H} = \frac{\boldsymbol{p}^2}{2m} + \mu_{\rm B} H \sigma \quad , \tag{2.8}$$

where $\mu_{\rm B}$ is the *Bohr magneton*,

$$\begin{aligned} \mu_{\rm B} &= \frac{e\hbar}{2mc} = 5.788 \times 10^{-9}\,{\rm eV/G} \\ \mu_{\rm B}/k_{\rm B} &= 6.717 \times 10^{-5}\,{\rm K/G} \quad , \end{aligned} \tag{2.9}$$

where m is the electron mass. What happens at $T = 0$ to a noninteracting electron gas in a magnetic field?

Electrons of each spin polarization form their own Fermi surfaces. That is, there is an up spin Fermi surface, with Fermi wavevector $k_{\rm F\uparrow}$, and a down spin Fermi surface, with Fermi wavevector $k_{\rm F\downarrow}$. The individual Fermi energies, on the other hand, must be equal, hence

$$\frac{\hbar^2 k_{\rm F\uparrow}^2}{2m} + \mu_{\rm B} H = \frac{\hbar^2 k_{\rm F\downarrow}^2}{2m} - \mu_{\rm B} H \quad , \tag{2.10}$$

which says

$$k_{\rm F\downarrow}^2 - k_{\rm F\uparrow}^2 = \frac{2eH}{\hbar c} \quad . \tag{2.11}$$

The total density is

$$n = \frac{k_{\rm F\uparrow}^3}{6\pi^2} + \frac{k_{\rm F\downarrow}^3}{6\pi^2} \qquad \Longrightarrow \qquad k_{\rm F\uparrow}^3 + k_{\rm F\downarrow}^3 = 6\pi^2 n \quad . \tag{2.12}$$

Clearly the down spin Fermi surface grows and the up spin Fermi surface shrinks with increasing H. Eventually, the minority spin Fermi surface vanishes altogether. This happens for the up spins when $k_{\rm F\uparrow} = 0$. Solving for the critical field, we obtain

$$H_{\rm c} = \frac{\hbar c}{2e} \cdot \left(6\pi^2 n\right)^{1/3} \quad . \tag{2.13}$$

In real magnetic solids, like cobalt and nickel, the spin-split Fermi surfaces are not spheres, just like the case of the (spin degenerate) Fermi surfaces for Cs and Y shown in fig. 2.1.

2.3 Quantum Thermodynamics of the Electron Gas

Electrons are fermions, and from this flows some universal features of their thermodynamic properties. We shall assume for the moment that the electrons are noninteracting, or that their mutual interactions can be treated within a "mean field" scheme. In this case, the grand potential of the electron gas is given by

$$\begin{aligned} \Omega(T, V, \mu) &= -V k_{\rm B} T \sum_\alpha \ln\Big(1 + e^{\mu/k_{\rm B}T}\, e^{-\varepsilon_\alpha/k_{\rm B}T}\Big) \\ &= -V k_{\rm B} T \int\limits_{-\infty}^{\infty} d\varepsilon\; g(\varepsilon)\; \ln\Big(1 + e^{(\mu-\varepsilon)/k_{\rm B}T}\Big) \quad . \end{aligned} \tag{2.14}$$

The average number of particles in a state with energy ε is

$$n(\varepsilon) = \frac{1}{e^{(\varepsilon-\mu)/k_{\rm B}T} + 1} \quad , \tag{2.15}$$

hence the total number of particles is

$$N = V \int\limits_{-\infty}^{\infty} d\varepsilon\; g(\varepsilon)\, \frac{1}{e^{(\varepsilon-\mu)/k_{\rm B}T} + 1} \quad . \tag{2.16}$$

2.3.1 Fermi distribution

We define the function $f(x) = 1/(e^{\beta x} + 1)$, known as the *Fermi distribution*. In the $T \to \infty$ limit, $f(\epsilon) \to \frac{1}{2}$ for all finite values of ε. As $T \to 0$, $f(\epsilon)$ approaches a step function $\Theta(-\epsilon)$. The average number of particles in a state of energy ε in a system at temperature T and chemical potential μ is $n(\varepsilon) = f(\varepsilon - \mu)$. In fig. 2.5 we plot $f(\varepsilon - \mu)$ *versus* ε for three representative temperatures.

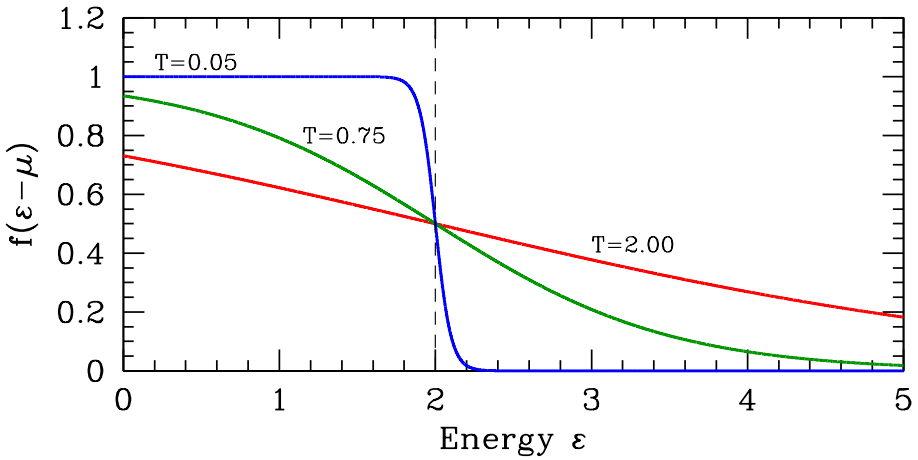

Figure 2.5: The Fermi distribution, $f(\varepsilon-\mu) = \left[\exp\left((\varepsilon-\mu)/k_{\rm B}T\right)+1\right]^{-1}$. Here we have set $k_{\rm B}=1$ and taken $\mu = 2$, with $T = \frac{1}{20}$ (blue), $T = \frac{3}{4}$ (green), and $T = 2$ (red). In the $T \to 0$ limit, $f(\varepsilon-\mu)$ approaches a step function $\Theta(\mu-\varepsilon)$.

2.3.2 Sommerfeld expansion

In dealing with the ideal Fermi gas, we will repeatedly encounter integrals of the form

$$\mathcal{I}(T,\mu) \equiv \int\limits_{-\infty}^{\infty} d\varepsilon\; f(\varepsilon-\mu)\,\phi(\varepsilon)\;. \tag{2.17}$$

The Sommerfeld expansion provides a systematic way of expanding these expressions in powers of T and is an important analytical tool in analyzing the low temperature properties of the ideal Fermi gas (IFG). We start by defining

$$\Phi(\varepsilon) \equiv \int\limits_{-\infty}^{\varepsilon} d\varepsilon'\;\phi(\varepsilon') \tag{2.18}$$

so that $\phi(\varepsilon) = \Phi'(\varepsilon)$. We then have

$$\mathcal{I} = \int\limits_{-\infty}^{\infty} d\varepsilon\; f(\varepsilon-\mu)\,\frac{d\Phi}{d\varepsilon} = -\int\limits_{-\infty}^{\infty} d\varepsilon\; f'(\varepsilon)\,\Phi(\mu+\varepsilon)\;, \tag{2.19}$$

where we assume $\Phi(-\infty) = 0$. Next, we invoke Taylor's theorem, to write

$$\Phi(\mu+\varepsilon) = \sum_{n=0}^{\infty} \frac{\varepsilon^n}{n\,!}\,\frac{d^n\Phi}{d\mu^n} = \exp\left(\varepsilon\,\frac{d}{d\mu}\right)\,\Phi(\mu)\;. \tag{2.20}$$

This last expression involving the exponential of a differential operator may appear overly formal but it proves extremely useful. Since

$$f'(\varepsilon) = -\frac{1}{k_{\rm B}T}\,\frac{e^{\varepsilon/k_{\rm B}T}}{\left(e^{\varepsilon/k_{\rm B}T}+1\right)^2}\quad, \tag{2.21}$$

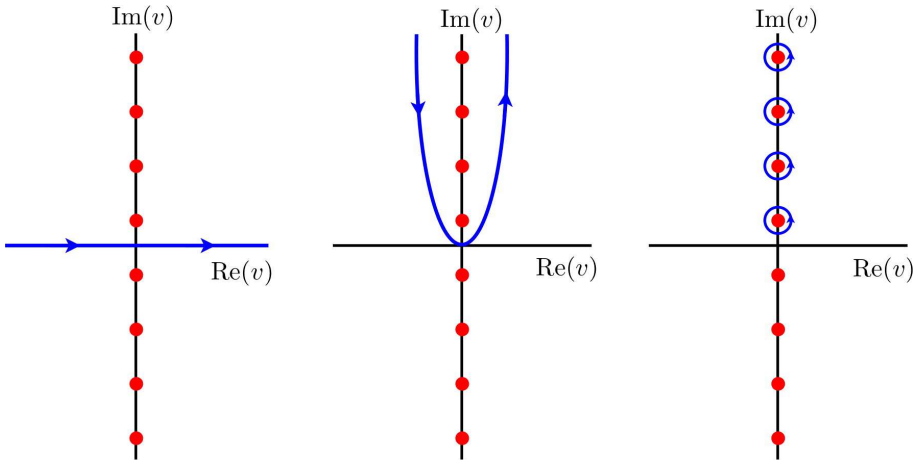

Figure 2.6: Deformation of the complex integration contour in eqn. 2.23.

we can write

$$\mathcal{I} = \int\limits_{-\infty}^{\infty} dv \, \frac{e^{vD}}{(e^v+1)(e^{-v}+1)} \, \Phi(\mu) \quad , \tag{2.22}$$

with $v = \varepsilon/k_{\rm B}T$, where $D = k_{\rm B}T\,\frac{d}{d\mu}$ is a dimensionless differential operator. The integral can now be done using the methods of complex integration:[2]

$$\begin{aligned}\int\limits_{-\infty}^{\infty} dv \, \frac{e^{vD}}{(e^v+1)(e^{-v}+1)} &= 2\pi i \sum_{n=1}^{\infty} \mathrm{Res}\left[\frac{e^{vD}}{(e^v+1)(e^{-v}+1)}\right]_{v=(2n+1)i\pi} \\ &= -2\pi i \sum_{n=0}^{\infty} D\, e^{(2n+1)i\pi D} = -\frac{2\pi i D\, e^{i\pi D}}{1-e^{2\pi i D}} = \pi D\, \csc \pi D \quad .\end{aligned} \tag{2.23}$$

Thus,

$$\mathcal{I}(T,\mu) = \pi D \csc(\pi D)\, \Phi(\mu) \, , \tag{2.24}$$

which is to be understood as the differential operator $\pi D \csc(\pi D) = \pi D/\sin(\pi D)$ acting on the function $\Phi(\mu)$. Appealing once more to Taylor's theorem, we have

$$\pi D \csc(\pi D) = 1 + \frac{\pi^2}{6}\,(k_{\rm B}T)^2\,\frac{d^2}{d\mu^2} + \frac{7\pi^4}{360}\,(k_{\rm B}T)^4\,\frac{d^4}{d\mu^4} + \ldots \, . \tag{2.25}$$

Thus,

$$\mathcal{I}(T,\mu) = \int\limits_{-\infty}^{\infty} d\varepsilon \, f(\varepsilon-\mu)\,\phi(\varepsilon) = \int\limits_{-\infty}^{\mu} d\varepsilon \, \phi(\varepsilon) + \frac{\pi^2}{6}\,(k_{\rm B}T)^2\,\phi'(\mu) + \frac{7\pi^4}{360}\,(k_{\rm B}T)^4\,\phi'''(\mu) + \ldots \, . \tag{2.26}$$

[2]Note that writing $v = (2n+1)\,i\pi + \epsilon$ we have $e^{\pm v} = -1 \mp \epsilon - \frac{1}{2}\epsilon^2 + \ldots$, so $(e^v+1)(e^{-v}+1) = -\epsilon^2 + \ldots$ We then expand $e^{vD} = e^{(2n+1)i\pi D}\big(1 + \epsilon D + \ldots\big)$ to find the residue: $\mathrm{Res} = -D\,e^{(2n+1)i\pi D}$.

If $\phi(\varepsilon)$ is a polynomial function of its argument, then each derivative effectively reduces the order of the polynomial by one degree, and the dimensionless parameter of the expansion is $(T/\mu)^2$. This procedure is known as the *Sommerfeld expansion*.

2.3.3 Chemical potential shift

As our first application of the Sommerfeld expansion formalism, let us compute $\mu(n,T)$ for the ideal Fermi gas. The number density $n(T,\mu)$ is

$$n = \int\limits_{-\infty}^{\infty} d\varepsilon\, g(\varepsilon)\, f(\varepsilon-\mu) = \int\limits_{-\infty}^{\mu} d\varepsilon\, g(\varepsilon) + \frac{\pi^2}{6}\,(k_{\rm B}T)^2\, g'(\mu) + \dots\ . \tag{2.27}$$

Let us write $\mu = \varepsilon_{\rm F} + \delta\mu$, where $\varepsilon_{\rm F} = \mu(T=0,n)$ is the Fermi energy, which is the chemical potential at $T=0$. We then have

$$\begin{aligned} n &= \int\limits_{-\infty}^{\varepsilon_{\rm F}+\delta\mu} d\varepsilon\, g(\varepsilon) + \frac{\pi^2}{6}\,(k_{\rm B}T)^2\, g'(\varepsilon_{\rm F}+\delta\mu) + \dots \\ &= \int\limits_{-\infty}^{\varepsilon_{\rm F}} d\varepsilon\, g(\varepsilon) + g(\varepsilon_{\rm F})\,\delta\mu + \frac{\pi^2}{6}\,(k_{\rm B}T)^2\, g'(\varepsilon_{\rm F}) + \dots\ , \end{aligned} \tag{2.28}$$

from which we derive

$$\delta\mu = -\frac{\pi^2}{6}\,(k_{\rm B}T)^2\,\frac{g'(\varepsilon_{\rm F})}{g(\varepsilon_{\rm F})} + \mathcal{O}(T^4)\ . \tag{2.29}$$

Note that $g'/g = (\ln g)'$. For a ballistic dispersion, assuming g = 2,

$$g(\varepsilon) = 2\int \frac{d^3k}{(2\pi)^3}\,\delta\!\left(\varepsilon - \frac{\hbar^2k^2}{2m}\right) = \left.\frac{m\,k(\varepsilon)}{\pi^2\hbar^2}\right|_{k(\varepsilon)=\frac{1}{\hbar}\sqrt{2m\varepsilon}} \tag{2.30}$$

Thus, $g(\varepsilon) \propto \varepsilon^{1/2}$ and $(\ln g)' = \frac{1}{2}\,\varepsilon^{-1}$, so

$$\mu(n,T) = \varepsilon_{\rm F} - \frac{\pi^2}{12}\,\frac{(k_{\rm B}T)^2}{\varepsilon_{\rm F}} + \dots\ , \tag{2.31}$$

where $\varepsilon_{\rm F}(n) = \frac{\hbar^2}{2m}(3\pi^2 n)^{2/3}$.

2.3.4 Specific heat

The energy of the electron gas is

$$\begin{aligned}\frac{E}{V} &= \int\limits_{-\infty}^{\infty} d\varepsilon\, g(\varepsilon)\,\varepsilon\, f(\varepsilon-\mu) = \int\limits_{-\infty}^{\mu} d\varepsilon\, g(\varepsilon)\,\varepsilon + \frac{\pi^2}{6}\,(k_{\rm B}T)^2\,\frac{d}{d\mu}\Big(\mu\, g(\mu)\Big) + \ldots \\ &= \int\limits_{-\infty}^{\varepsilon_{\rm F}} d\varepsilon\, g(\varepsilon)\,\varepsilon + g(\varepsilon_{\rm F})\,\varepsilon_{\rm F}\,\delta\mu + \frac{\pi^2}{6}\,(k_{\rm B}T)^2\,\varepsilon_{\rm F}\,g'(\varepsilon_{\rm F}) + \frac{\pi^2}{6}\,(k_{\rm B}T)^2\,g(\varepsilon_{\rm F}) + \ldots \\ &= {\rm e}_0 + \frac{\pi^2}{6}\,(k_{\rm B}T)^2\,g(\varepsilon_{\rm F}) + \ldots\ ,\end{aligned} \tag{2.32}$$

where

$$ {\rm e}_0 = \int\limits_{-\infty}^{\varepsilon_{\rm F}} d\varepsilon\, g(\varepsilon)\,\varepsilon \tag{2.33}$$

is the ground state energy density (*i.e.* ground state energy per unit volume). Thus,

$$ C_{V,N} = \left(\frac{\partial E}{\partial T}\right)_{V,N} = \frac{\pi^2}{3}\,V k_{\rm B}^2\,T\,g(\varepsilon_{\rm F}) \equiv V\gamma\,T\ , \tag{2.34}$$

where

$$ \gamma = \frac{\pi^2}{3}\,k_{\rm B}^2\,g(\varepsilon_{\rm F})\ . \tag{2.35}$$

Note that the molar heat capacity is

$$ c_V = \frac{N_{\rm A}}{N}\cdot C_V = \frac{\pi^2}{3}R\cdot\frac{k_{\rm B}T\,g(\varepsilon_{\rm F})}{n} = \frac{\pi^2}{2}\left(\frac{k_{\rm B}T}{\varepsilon_{\rm F}}\right)R\ , \tag{2.36}$$

where in the last expression on the RHS we have assumed a ballistic dispersion, for which

$$ \frac{g(\varepsilon_{\rm F})}{n} = \frac{{\rm g}\,mk_{\rm F}}{2\pi^2\hbar^2}\cdot\frac{6\pi^2}{{\rm g}\,k_{\rm F}^3} = \frac{3}{2\,\varepsilon_{\rm F}}\ . \tag{2.37}$$

The molar heat capacity in eqn. 2.36 is to be compared with the classical ideal gas value of $\frac{3}{2}R$. Relative to the classical ideal gas, the IFG value is reduced by a fraction of $(\pi^2/3)\times(k_{\rm B}T/\varepsilon_{\rm F})$, which in most metals is very small and even at room temperature is only on the order of 10^{-2}. Most of the heat capacity of metals at room temperature is due to the energy stored in lattice vibrations.

2.4 Effects of External Magnetic Fields

2.4.1 Magnetic susceptibility and Pauli paramagnetism

Magnetism has two origins: (i) orbital currents of charged particles, and (ii) intrinsic magnetic moment. The intrinsic magnetic moment $\boldsymbol{m}$ of a particle is related to its quantum mechanical *spin* via

$$ \boldsymbol{m} = \tilde{g}\mu_0\boldsymbol{S}/\hbar \qquad , \qquad \mu_0 = \frac{q\hbar}{2mc} = \text{magneton}\ , \tag{2.38}$$

where $\tilde{g}$ is the particle's g-factor[3], μ_0 its magnetic moment, and $\boldsymbol{S}$ is the vector of quantum mechanical spin operators satisfying $\left[S^\alpha\,,\,S^\beta\right] = i\hbar\epsilon_{\alpha\beta\gamma}\,S^\gamma$, *i.e.* SU(2) commutation relations. The Hamiltonian for a single particle is then

$$\hat{H} = \frac{1}{2m^*}\Big(\boldsymbol{p} - \frac{q}{c}\boldsymbol{A}\Big)^2 - \boldsymbol{H}\cdot\boldsymbol{m} = \frac{1}{2m^*}\Big(\boldsymbol{p} + \frac{e}{c}\boldsymbol{A}\Big)^2 + \tfrac{1}{2}\tilde{g}\,\mu_{\rm B}H\,\sigma\ , \tag{2.39}$$

where in the last line we've restricted our attention to the electron, for which $q = -e$. The g-factor for an electron is $\tilde{g} = 2$ at tree level, and when radiative corrections are accounted for using quantum electrodynamics (QED) one finds $\tilde{g} = 2.0023193043617(15)$. For our purposes we can take $\tilde{g} = 2$, although we can always absorb the small difference into the definition of $\mu_{\rm B}$, writing $\mu_{\rm B} \to \tilde{\mu}_{\rm B} = \tilde{g}e\hbar/4mc$. We've chosen the $\hat{z}$-axis in spin space to point in the direction of the magnetic field, and we wrote the eigenvalues of S^z as $\frac{1}{2}\hbar\sigma$, where $\sigma = \pm 1$. The quantity m^* is the *effective mass* of the electron, here assumed to be isotropic in the vicinity of a band edge. An important distinction is that it is m^* which enters into the kinetic energy term $\boldsymbol{p}^2/2m^*$, but it is the electron mass m itself ($m = 511\,\text{keV}$) which enters into the definition of the Bohr magneton. We shall discuss the consequences of this further below.

In a crystalline semiconductor, the spin-orbit interaction,

$$V_{\rm so} = \frac{\hbar}{4m^2c^2}\,\boldsymbol{p}\cdot\boldsymbol{\sigma}\times\boldsymbol{\nabla}V \quad , \tag{2.40}$$

leads to an effective $\tilde{g}$ which is often very far from the free electron value. For cubic systems with a direct band gap, the g-factor in band n is given by[4]

$$\frac{\tilde{g}}{2} = 1 + \frac{2}{m}\,\mathsf{Im}\sum_{n'}{}'\frac{\langle\, n\,\Gamma\,|\,p_x\,|\,n'\,\Gamma\,\rangle\langle\, n'\,\Gamma\,|\,p_y\,|\,n\,\Gamma\,\rangle}{E_n(\Gamma) - E_{n'}(\Gamma)} + \ldots \quad , \tag{2.41}$$

where the wavefunctions and the energies are all taken at the zone center Γ. InSb, for example, has $\tilde{g} \simeq -44$, while in GaAs $\tilde{g} \simeq 0.4$.

In the absence of orbital magnetic coupling, the single particle dispersion is

$$\varepsilon_\sigma(\boldsymbol{k}) = \frac{\hbar^2\boldsymbol{k}^2}{2m^*} + \tilde{\mu}_{\rm B}H\,\sigma\ . \tag{2.42}$$

At $T = 0$, we have the results of §2.2.3. At finite T, we once again use the Sommerfeld expansion. We then have

$$\begin{aligned} n &= \int\limits_{-\infty}^{\infty} d\varepsilon\; g_\uparrow(\varepsilon)\,f(\varepsilon-\mu) \;+\; \int\limits_{-\infty}^{\infty} d\varepsilon\; g_\downarrow(\varepsilon)\,f(\varepsilon-\mu) \\ &= \tfrac{1}{2}\int\limits_{-\infty}^{\infty} d\varepsilon\,\Big\{g(\varepsilon-\tilde{\mu}_{\rm B}H) + g(\varepsilon+\tilde{\mu}_{\rm B}H)\Big\}\,f(\varepsilon-\mu) \\ &= \int\limits_{-\infty}^{\infty} d\varepsilon\,\Big\{g(\varepsilon) + (\tilde{\mu}_{\rm B}H)^2\,g''(\varepsilon) + \ldots\Big\}\,f(\varepsilon-\mu)\ . \end{aligned} \tag{2.43}$$

[3]We denote the g-factor by $\tilde{g}$ in order to obviate confusion with the density of states function $g(\varepsilon)$.

[4]See, *e.g.*, ch. 14 of C. Kittel, *Quantum Theory of Solids*.

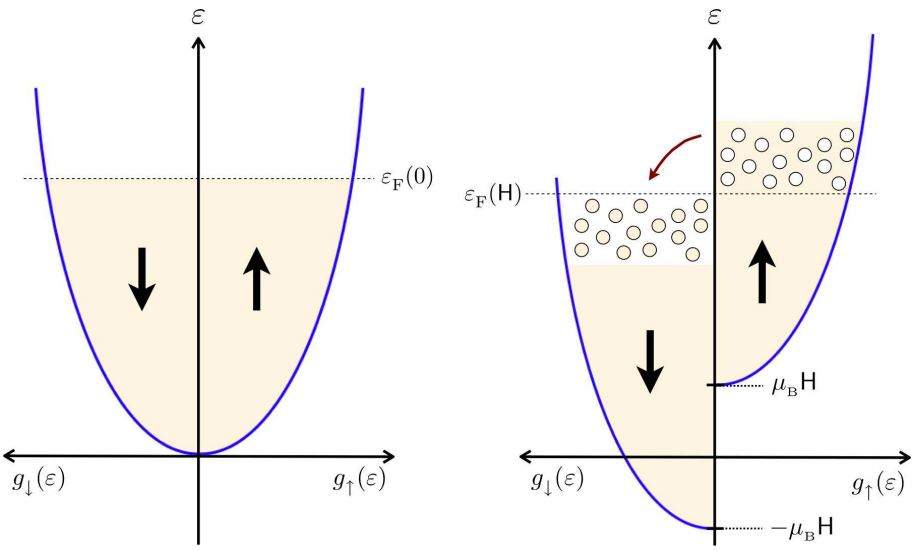

Figure 2.7: Fermi distributions in the presence of an external Zeeman-coupled magnetic field.

We now invoke the Sommerfeld expension to find the temperature dependence:

$$\begin{aligned} n &= \int\limits_{-\infty}^{\mu} d\varepsilon\, g(\varepsilon) + \frac{\pi^2}{6}\,(k_{\rm B}T)^2\,g'(\mu) + (\tilde\mu_{\rm B}H)^2\,g'(\mu) + \dots \\ &= \int\limits_{-\infty}^{\varepsilon_{\rm F}} d\varepsilon\, g(\varepsilon) + g(\varepsilon_{\rm F})\,\delta\mu + \frac{\pi^2}{6}\,(k_{\rm B}T)^2\,g'(\varepsilon_{\rm F}) + (\tilde\mu_{\rm B}H)^2\,g'(\varepsilon_{\rm F}) + \dots\ . \end{aligned} \tag{2.44}$$

Note that the density of states for spin species σ is

$$g_\sigma(\varepsilon) = \tfrac{1}{2}\,g(\varepsilon - \tilde\mu_{\rm B}H\sigma)\ , \tag{2.45}$$

where $g(\varepsilon)$ is the total density of states per unit volume, for both spin species, in the absence of a magnetic field. We conclude that the chemical potential shift in an external field is

$$\delta\mu(T,n,H) = -\left\{\frac{\pi^2}{6}\,(k_{\rm B}T)^2 + (\tilde\mu_{\rm B}H)^2\right\}\frac{g'(\varepsilon_{\rm F})}{g(\varepsilon_{\rm F})} + \dots\ . \tag{2.46}$$

We next compute the difference $n_\uparrow - n_\downarrow$ in the densities of up and down spin electrons:

$$\begin{aligned} n_\uparrow - n_\downarrow &= \int\limits_{-\infty}^{\infty} d\varepsilon\,\Big\{g_\uparrow(\varepsilon) - g_\downarrow(\varepsilon)\Big\}\,f(\varepsilon-\mu) \\ &= \tfrac{1}{2}\int\limits_{-\infty}^{\infty} d\varepsilon\,\Big\{g(\varepsilon-\tilde\mu_{\rm B}H) - g(\varepsilon+\tilde\mu_{\rm B}H)\Big\}\,f(\varepsilon-\mu) \\ &= -\tilde\mu_{\rm B}H\cdot\pi D\csc(\pi D)\,g(\mu) + \mathcal{O}(H^3)\ . \end{aligned} \tag{2.47}$$

We needn't go beyond the trivial lowest order term in the Sommerfeld expansion, because H is already assumed to be small. Thus, the magnetization density is

$$M = -\tilde{\mu}_{\rm B}(n_\uparrow - n_\downarrow) = \tilde{\mu}_{\rm B}^2\, g(\varepsilon_{\rm F})\, H \ . \tag{2.48}$$

in which the magnetic susceptibility is

$$\chi = \left(\frac{\partial M}{\partial H}\right)_{T,N} = \tilde{\mu}_{\rm B}^2\, g(\varepsilon_{\rm F}) \ . \tag{2.49}$$

This is called the *Pauli paramagnetic susceptibility*.

2.4.2 Landau diamagnetism

When orbital effects are included, the single particle energy levels are given by

$$\varepsilon(n, k_z, \sigma) = (n + \tfrac{1}{2})\hbar\omega_{\rm c} + \frac{\hbar^2 k_z^2}{2m^*} + \tilde{\mu}_{\rm B} H\, \sigma \ . \tag{2.50}$$

Here n is a Landau level index, and $\omega_{\rm c} = eH/m^*c$ is the *cyclotron frequency*. Note that

$$\frac{\tilde{\mu}_{\rm B} H}{\hbar\omega_{\rm c}} = \frac{ge\hbar H}{4mc} \cdot \frac{m^* c}{\hbar e H} = \frac{\tilde{g}}{4} \cdot \frac{m^*}{m} \ . \tag{2.51}$$

Accordingly, we define the ratio $r \equiv (\tilde{g}/2) \times (m^*/m)$. We can then write

$$\varepsilon(n, k_z, \sigma) = \big(n + \tfrac{1}{2} + \tfrac{1}{2} r\sigma\big)\hbar\omega_{\rm c} + \frac{\hbar^2 k_z^2}{2m^*} \ . \tag{2.52}$$

The density of states per unit volume is then

$$g(\varepsilon) = \frac{1}{2\pi\ell^2} \sum_{n,\sigma} \int\limits_{-\infty}^{\infty} \frac{dk_z}{2\pi}\, \delta\big(\varepsilon - \varepsilon(n, k_z, \sigma)\big) \quad , \tag{2.53}$$

where $\ell = (\hbar c/eH)^{1/2}$ is the *magnetic length*. The significance of ℓ is that the area per Dirac fluxoid $\phi_0 = hc/e$ is $2\pi\ell^2$.

The grand potential is then given by

$$\Omega = -\frac{HA}{\phi_0} \cdot L_z \cdot k_{\rm B}T \int\limits_{-\infty}^{\infty} \frac{dk_z}{2\pi} \sum_{n=0}^{\infty} \sum_{\sigma=\pm 1} \ln\Big[1 + e^{\mu/k_{\rm B}T}\, e^{-(n+\frac{1}{2}+\frac{1}{2}r\sigma)\,\hbar\omega_{\rm c}/k_{\rm B}T}\, e^{-\hbar^2 k_z^2/2m^* k_{\rm B}T}\Big] \ . \tag{2.54}$$

A few words are in order here regarding the prefactor. In the presence of a uniform magnetic field, the energy levels of a two-dimensional ballistic charged particle collapse into Landau levels. The number of states per Landau level scales with the area of the system, and is equal to the number of flux quanta through the system: $N_\phi = HA/\phi_0$, where $\phi_0 = hc/e$ is the Dirac flux quantum. Note that

$$\frac{HA}{\phi_0} \cdot L_z \cdot k_{\rm B}T = \hbar\omega_{\rm c} \cdot \frac{V}{\lambda_T^3} \ , \tag{2.55}$$

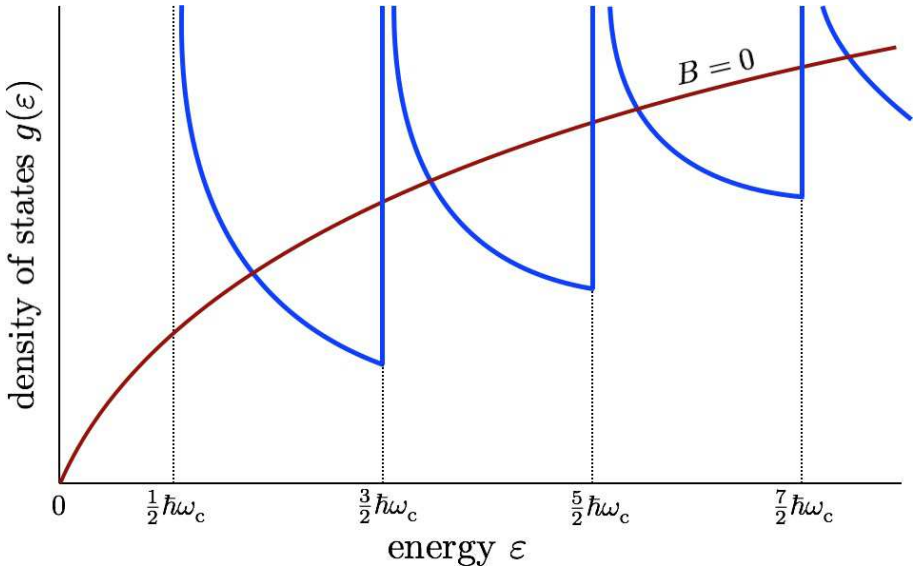

Figure 2.8: Density of states for a three-dimensional free electron gas with $\tilde{g} = 0$ in the presence of an external magnetic field (blue), compared with $B = 0$ result (dark red).

hence we can write

$$\Omega(T, V, \mu, H) = \hbar\omega_c \sum_{n=0}^{\infty} \sum_{\sigma=\pm 1} Q\big((n + \tfrac{1}{2} + \tfrac{1}{2} r\sigma)\,\hbar\omega_c - \mu\big)\ , \tag{2.56}$$

where we have defined the dimensionless function

$$Q(\varepsilon) = -\frac{V}{\lambda_T^2} \int_{-\infty}^{\infty} \frac{dk_z}{2\pi}\ \ln\Big[1 + e^{-\varepsilon/k_B T} e^{-\hbar^2 k_z^2/2m^* k_B T}\Big]\ . \tag{2.57}$$

We now invoke the Euler-MacLaurin formula,

$$\sum_{n=0}^{\infty} F(n) = \int_0^{\infty} dx\ F(x) + \tfrac{1}{2}\,F(0) - \tfrac{1}{12}\,F'(0) + \dots\ , \tag{2.58}$$

resulting in

$$\Omega(T, V, \mu, H) = \sum_{\sigma=\pm 1} \left\{ \int_{\frac{1}{2}(1+r\sigma)\hbar\omega_c}^{\infty} d\varepsilon\, Q(\varepsilon - \mu) + \tfrac{1}{2}\,\hbar\omega_c\, Q\big(\tfrac{1}{2}(1 + r\sigma)\,\hbar\omega_c - \mu\big) \right. \\ \left. - \tfrac{1}{12}\,(\hbar\omega_c)^2\, Q'\big(\tfrac{1}{2}(1 + r\sigma)\,\hbar\omega_c - \mu\big) + \dots \right\}\ . \tag{2.59}$$

We next expand in powers of the magnetic field H to obtain

$$\Omega(T,V,\mu,H) = 2\int\limits_0^\infty d\varepsilon\, Q(\varepsilon-\mu) + \tfrac{1}{4}\big(r^2-\tfrac{1}{3}\big)\,(\hbar\omega_{\rm c})^2\,Q'(-\mu) + \ldots\ . \tag{2.60}$$

Thus, the magnetic susceptibility is

$$\begin{aligned}\chi &= -\frac{1}{V}\frac{\partial^2\Omega}{\partial H^2} = \big(r^2-\tfrac{1}{3}\big)\cdot\tilde\mu_{\rm B}^2\cdot\big(m/m^*\big)^2\cdot\Big(-\frac{2}{V}\,Q'(-\mu)\Big) \\ &= \left(\frac{\tilde g^2}{4}-\frac{m^2}{3m^{*2}}\right)\cdot\tilde\mu_{\rm B}^2\cdot n^2\kappa_T\ ,\end{aligned} \tag{2.61}$$

where κ_T is the isothermal compressibility[5], which at $T=0$ is related to the density of states by $\kappa_T(T=0,n) = n^{-2}g(\varepsilon_{\rm F})$. In most metals we have $m^*\approx m$ and the term in brackets is positive (recall $\tilde g\approx 2$). In semiconductors, however, we can have $m^*\ll m$; for example in GaAs we have $m^*=0.067\,m$ and $\tilde g = 0.4$. Thus, semiconductors can have a *diamagnetic* response. If we take $\tilde g = 2$ and $m^*=m$, we see that the orbital currents give rise to a diamagnetic contribution to the magnetic susceptibility which is exactly $-\frac{1}{3}$ times as large as the contribution arising from Zeeman coupling. The net result is then paramagnetic ($\chi>0$) and $\frac{2}{3}$ as large as the Pauli susceptibility. The orbital currents can be understood within the context of *Lenz's law*.

2.4.3 de Haas-van Alphen oscillations

The Landau level structure in the density of states (see Fig. 2.8) is responsible for striking behavior in metals when subjected to an external magnetic field. For weak fields, the magnetization density is $m=\chi H$, but at stronger fields we have

$$\begin{aligned}m(T,H,\mu) = -\frac{1}{V}\,\frac{\partial\Omega}{\partial H} = \left(\frac{e^2}{4\pi^2\hbar}\right)\left(\frac{2\mu}{m^*}\right)^{1/2} H\cdot\Bigg\{\big(r^2-\tfrac{1}{3}\big) + \\ + \left(\frac{2\pi k_{\rm B}T}{\hbar\omega_{\rm c}}\right)\left(\frac{2\mu}{\hbar\omega_{\rm c}}\right)^{1/2}\sum_{l=1}^\infty\frac{(-1)^l}{\sqrt{l}}\,\frac{\sin\big(\frac{2\pi l\mu}{\hbar\omega_{\rm c}}-\frac{\pi}{4}\big)\cos\big(l\pi r\big)}{\sinh\big(2\pi^2 l k_{\rm B}T/\hbar\omega_{\rm c}\big)}\Bigg\}\ .\end{aligned} \tag{2.62}$$

The electron number density is given by

$$\begin{aligned}n(T,H,\mu) = -\frac{1}{V}\,\frac{\partial\Omega}{\partial\mu} = \frac{1}{3\pi^2}\left(\frac{2m^*\mu}{\hbar^2}\right)^{1/2}\cdot\Bigg\{1+\frac{3}{32}\left(\frac{\hbar\omega_{\rm c}}{\mu}\right)\big(r^2-\tfrac{1}{3}\big) + \\ + \left(\frac{3\pi k_{\rm B}T}{\hbar\omega_{\rm c}}\right)\left(\frac{\hbar\omega_{\rm c}}{2\mu}\right)^{3/2}\sum_{l=1}^\infty\frac{(-1)^l}{\sqrt{l}}\,\frac{\sin\big(\frac{2\pi l\mu}{\hbar\omega_{\rm c}}-\frac{\pi}{4}\big)\cos\big(l\pi r\big)}{\sinh\big(2\pi^2 l k_{\rm B}T/\hbar\omega_{\rm c}\big)}\Bigg\}\ .\end{aligned} \tag{2.63}$$

These expressions are valid in the limit $\mu\gg\hbar\omega_{\rm c}$ and $\mu\gg k_{\rm B}T$. Under experimental conditions, it is the electron number density n which is held constant, and not the chemical potential μ. Thus, one must invert to obtain $\mu(n,T,H)$ and substitute this in the expression for $m(T,H,\mu)$ to obtain $m(n,T,H)$.

[5] We've used $-\frac{2}{V}\,Q'(\mu) = -\frac{1}{V}\frac{\partial^2\Omega}{\partial\mu^2} = n^2\kappa_T$.

To derive the above results, we integrate Eqn. 2.14 twice by parts to obtain

$$\Omega = -V \int\limits_{-\infty}^{\infty} d\varepsilon \, R(\varepsilon) \left(-\frac{\partial f}{\partial \varepsilon} \right) \quad , \tag{2.64}$$

where $R(\varepsilon)$ is given by

$$R(\varepsilon) = \int\limits_{-\infty}^{\varepsilon} d\varepsilon' \int\limits_{-\infty}^{\varepsilon'} d\varepsilon'' \, g(\varepsilon'') \quad , \tag{2.65}$$

i.e. $g(\varepsilon) = R''(\varepsilon)$. In the presence of a uniform magnetic field, the density of states for a ballistic particle with dispersion $\varepsilon(\boldsymbol{k}) = \hbar^2 \boldsymbol{k}^2 / 2m^*$ is

$$g(\varepsilon) = \frac{1}{2\pi\ell^2} \frac{\sqrt{m^*}}{\sqrt{2}\,\pi\hbar} \sum_{n=0}^{\infty} \sum_{\sigma=\pm 1} \Big[\varepsilon - \big(n + \tfrac{1}{2} + \tfrac{1}{2}\sigma r\big)\hbar\omega_{\rm c} \Big]_+^{-1/2} \quad , \tag{2.66}$$

where $r = \tilde{g}\, m^*/2m$ as before, and $[x]_+ \equiv x\,\Theta(x)$. Thus,

$$R(\varepsilon) = \frac{\sqrt{2}}{3\pi^2} \left(\frac{m^*}{\hbar^2} \right)^{3/2} \sum_{n=0}^{\infty} \sum_{\sigma=\pm 1} \Big[\varepsilon - \big(n + \tfrac{1}{2} + \tfrac{1}{2}\sigma r\big)\hbar\omega_{\rm c} \Big]_+^{3/2} \quad , \tag{2.67}$$

We now invoke the result

$$\sum_{n=0}^{\infty} \phi(n + \tfrac{1}{2}) = \int\limits_0^{\infty} du\, \phi(u) + \tfrac{1}{24}\phi'(0) - \sum_{n=1}^{\infty} \frac{(-1)^l}{2\pi^2 l^2} \int\limits_0^{\infty} du\, \phi''(u) \cos(2\pi l u) \quad , \tag{2.68}$$

which is valid provided $\phi(\infty) = \phi'(\infty) = 0$. This follows from applying the Poisson summation formula[6],

$$\sum_{n=-\infty}^{\infty} \delta(x - n) = \sum_{l=-\infty}^{\infty} e^{2\pi i l x} \quad , \tag{2.69}$$

integrating by parts twice, and using $\sum_{l=1}^{\infty} (-1)^{l+1} / \, l^2 = \frac{\pi^2}{12}$.

$$\begin{aligned} R(\varepsilon) = \frac{2\sqrt{2}}{15\pi^2} \left(\frac{m^*}{\hbar^2} \right)^{3/2} \frac{\big[\, \varepsilon - \frac{1}{2} r\hbar\omega_{\rm c} \,\big]_+^{5/2}}{\hbar\omega_{\rm c}} - \frac{\sqrt{2}}{48\pi^2} \left(\frac{m^*}{\hbar^2} \right)^{3/2} \hbar\omega_{\rm c} \, \big[\, \varepsilon - \tfrac{1}{2} r\hbar\omega_{\rm c} \,\big]_+^{3/2} + \\ - \frac{1}{8\pi^4} \left(\frac{m^*}{\hbar^2} \right)^{3/2} (\hbar\omega_{\rm c})^{3/2} \sum_{l=1}^{\infty} \frac{(-1)^l}{l^{5/2}} \cos\left(\frac{2\pi l \varepsilon}{\hbar\omega_{\rm c}} - \pi l r \sigma - \frac{\pi}{4} \right) \quad . \end{aligned} \tag{2.70}$$

We next integrate over ε, using the Sommerfeld expansion and the result

$$\int\limits_{-\infty}^{\infty} d\varepsilon \, e^{is\varepsilon} \left(-\frac{\partial f}{\partial \varepsilon} \right) = \frac{\pi s \, k_{\rm B} T}{\sinh(\pi s \, k_{\rm B} T)} \quad . \tag{2.71}$$

[6]One first extends the function $\phi(u)$ to the entire real line, symmetrically, so $\phi(-u) = \phi(u)$.

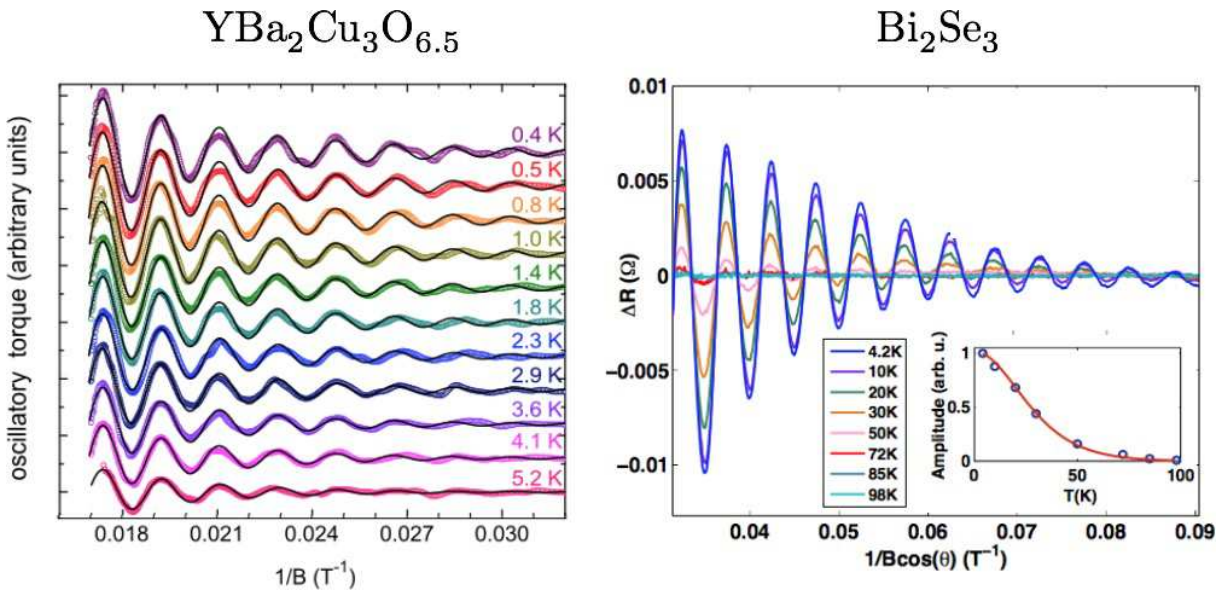

Figure 2.9: Left: de Haas-van Alphen oscillations in the underdoped high temperature superconductor $YBa_2Cu_3O_{6.5}$, measured by C. Jaudet *et al* in *Phys. Rev. Lett.* **100**, 187005 (2008). Right: Schubnikov-de Haas oscillations and their temperature dependence in the three-dimensional topological insulator Bi_2Se_3, indicating the presence of metallic surface states. A smooth polynomial background has been subtracted. Measurements by M. Petrushevsky *et al.* in *Phys. Rev. B* **86**, 045131 (2013).

The final result for $\Omega(T, V, \mu, H)$, valid for $\hbar\omega_{\rm c} \ll \mu$ and $k_{\rm B}T \ll \mu$, is

$$\Omega(T,V,\mu,H) = -V\cdot\frac{\sqrt{2}}{\pi}\left(\frac{m^*}{\hbar^2}\right)^{3/2}\Biggl\{\tfrac{4}{15}\left\langle\varepsilon^{5/2}\right\rangle + \tfrac{1}{8}\left(\hbar\omega_{\rm c}\right)^2\left(r^2-\tfrac{1}{3}\right)\left\langle\varepsilon^{1/2}\right\rangle + \\ + \tfrac{1}{2\sqrt{2}}\left(\hbar\omega_{\rm c}\right)^{3/2}k_{\rm B}T\sum_{l=1}^{\infty}\frac{(-1)^l}{l^{3/2}}\,\frac{\cos\left(\frac{2\pi l\mu}{\hbar\omega_{\rm c}}-\frac{\pi}{4}\right)\cos\left(l\pi r\right)}{\sinh\left(2\pi^2 l k_{\rm B}T/\hbar\omega_{\rm c}\right)}\Biggr\} \quad . \tag{2.72}$$

Here, we have used the notation

$$\left\langle\psi(\varepsilon)\right\rangle \equiv \int_{-\infty}^{\infty} d\varepsilon\,\psi(\varepsilon)\left(-\frac{\partial f}{\partial\varepsilon}\right) \quad . \tag{2.73}$$

For homogeneous functions,

$$\left\langle\varepsilon^p\right\rangle = \mu^p + \tfrac{\pi^2}{6}\,p(p-1)\left(k_{\rm B}T\right)^2\mu^{p-2} + \mathcal{O}(T^4) \quad . \tag{2.74}$$

Differentiation of $\Omega(T, V, H)$ with respect to H and μ yields[7], respectively, the results in Eqns. 2.62 and 2.63. From Eqn. 2.72, we see that the oscillating factors are periodic in $1/H$ with periods $\Delta(1/H) = \hbar e/2\pi l\mu m^* c$. In experiments, the magnetization M is typically measured with a torque-magnetometer.

[7]The cyclotron energy $\hbar\omega_{\rm c} = \hbar eH/m^*c$ is linear in the magnetic field H. For $\mu \gg \hbar\omega_{\rm c} \gg k_{\rm B}T$, the dominant contribution to the magnetization comes from differentiating the cosine factor.

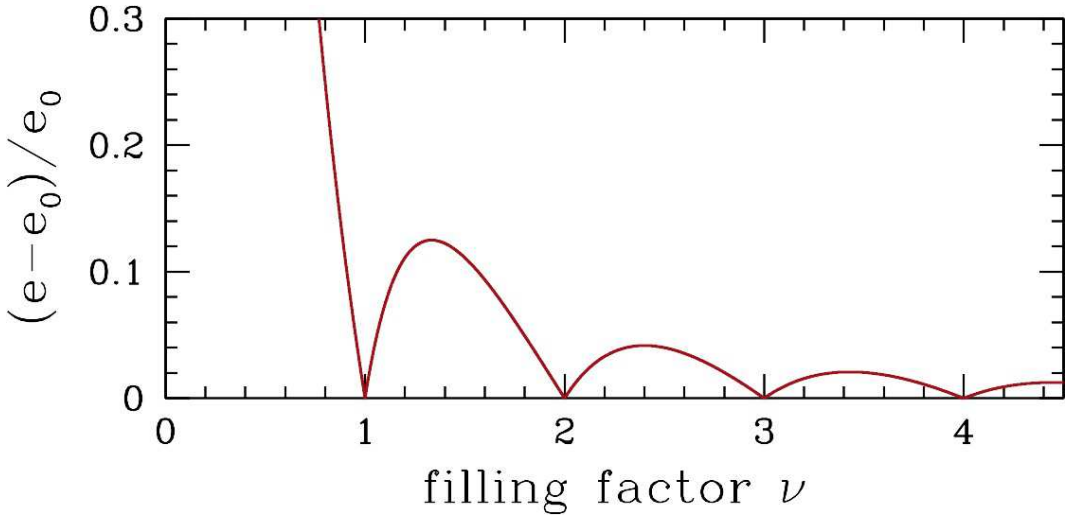

Figure 2.10: Two dimensional oscillations in the energy per unit area $e = E/A$ for a spinless electron gas in a uniform magnetic field $\boldsymbol{H} = H\hat{\boldsymbol{z}}$.

The oscillatory nature of $M(H)$ is called the de Haas-van Alphen effect. A related periodicity occurs in the magnetoresistance $R(H)$, where it is called the Schubnikov-de Haas effect. Experimental data for both effects is shown in Fig. 2.9.

Oscillations at $T = 0$: spinless fermions in $d = 2$ dimensions

Apparently the oscillations do not vanish, even at $T = 0$. The prefactor of T which multiplies the oscillating sum in Eqn. 2.62 cancels with the $\sinh(2\pi^2 l k_{\rm B} T/\hbar\omega_{\rm c})$ denominator in the $T \to 0$ limit. Consider the simple case of ballistic spinless electrons in $d = 2$ dimensions. We know that each Landau level can accommodate $N_{\rm L} = HA/\phi_0$ electrons, where $\phi_0 = hc/e$ is the Dirac flux quantum. It is convenient to define the *filling fraction* ν, as

$$\nu = \frac{N}{N_{\rm L}} = 2\pi\ell^2 n = \frac{2\pi\hbar c}{eH}\, n \quad , \tag{2.75}$$

where $\ell = \sqrt{\hbar c/eH}$ is the magnetic length. The cyclotron energy is

$$\hbar\omega_{\rm c} = \frac{\hbar eH}{m^* c} = \frac{2\pi\hbar^2}{m^*}\,\frac{n}{\nu} \quad . \tag{2.76}$$

We now evaluate the energy per unit area, $\mathrm{e} = E/A$, as a function of n and ν. With the electron number density n fixed, the magnetization per unit area is given by

$$m = \frac{\partial \mathrm{e}}{\partial H} = \frac{\partial \nu}{\partial H}\,\frac{\partial \mathrm{e}}{\partial \nu} = -\frac{\nu}{H}\,\frac{\partial \mathrm{e}}{\partial \nu} \quad . \tag{2.77}$$

Now if $\nu \in [j, j+1]$, the total energy is

$$\begin{aligned} E &= N_{\rm L} \cdot \tfrac{1}{2}\hbar\omega_{\rm c} \cdot \Big(1 + 3 + 5 + \ldots + (2j-1)\Big) + (N - jN_{\rm L}) \cdot (j + \tfrac{1}{2})\,\hbar\omega_{\rm c} \\ &= N_{\rm L} \cdot \tfrac{1}{2}\hbar\omega_{\rm c} \cdot \Big(j^2 + (\nu - j)(2j+1)\Big) \quad . \end{aligned} \tag{2.78}$$

Thus,

$$\mathrm{e}(n,\nu) = \frac{E}{A} = \frac{\pi\hbar^2 n^2}{m^*} \cdot \left\{ \frac{(2j+1)\,\nu - j(j+1)}{\nu^2} \right\} \quad . \tag{2.79}$$

Defining, $\mathrm{e}_0(n) = \pi\hbar^2 n^2/m^*$, we have that $\mathrm{e}(n,j) = \mathrm{e}(n,j+1) = \mathrm{e}_0(n)$. Furthermore, since

$$\left.\frac{\partial \mathrm{e}}{\partial \nu}\right|_{\nu=j} = \frac{\mathrm{e}_0(n)}{j^2} > 0 \qquad \text{and} \qquad \left.\frac{\partial \mathrm{e}}{\partial \nu}\right|_{\nu=j+1} = -\frac{\mathrm{e}_0(n)}{j^2} > 0 \quad , \tag{2.80}$$

we see that $\mathrm{e}(n,\nu)$ has a cusp at every integer value of ν. This behavior is depicted in Fig. 2.10. The magnetization density $m(n,\nu)$ therefore *discontinuously changes sign* (from negative to positive) across all integer values of the filling fraction![8] Note also that the periodicity is $\Delta\nu = 1$, hence

$$\Delta\Big(\frac{1}{H}\Big) = \frac{e}{hcn} = \frac{1}{2\pi n \phi_0} \quad . \tag{2.81}$$

2.4.4 de Haas-von Alphen effect for anisotropic Fermi surfaces

We consider a nontopological band structure, for which the semiclassical equations of motion in the presence of a uniform magnetic field are

$$\frac{d\boldsymbol{r}}{dt} = \boldsymbol{v}_n(\boldsymbol{k}) \qquad , \qquad \frac{d\boldsymbol{k}}{dt} = -\frac{e}{\hbar c}\,\boldsymbol{v}_n(\boldsymbol{k}) \times \boldsymbol{B} \quad . \tag{2.82}$$

These equations entail the conservation of the band energy $E_n(\boldsymbol{k})$:

$$\frac{dE_n(\boldsymbol{k})}{dt} = \frac{\partial E_n(\boldsymbol{k})}{\partial \boldsymbol{k}} \cdot \frac{d\boldsymbol{k}}{dt} = \hbar \boldsymbol{v}_n(\boldsymbol{k}) \cdot \left(-\frac{e}{\hbar c}\,\boldsymbol{v}_n(\boldsymbol{k}) \times \boldsymbol{B} \right) = 0 \quad . \tag{2.83}$$

Define $\boldsymbol{k}_\perp = \boldsymbol{k} - \widehat{\boldsymbol{B}}(\widehat{\boldsymbol{B}} \cdot \boldsymbol{k})$, the component of $\boldsymbol{k}$ along the direction $\widehat{\boldsymbol{B}}$. We then have $\dot{\boldsymbol{k}}_\perp = -\frac{e}{\hbar c}\,\boldsymbol{v}_n(\boldsymbol{k}) \times \boldsymbol{B}$ and $\frac{d}{dt}(\boldsymbol{k} \cdot \widehat{\boldsymbol{B}}) = 0$. Thus, the orbits $\boldsymbol{k}(t)$ lie in planes perpendicular to $\widehat{\boldsymbol{B}}$ (see the sketch in Fig. 2.11).

Consider now the differential $\boldsymbol{k}$-space area element $d^2k_\perp$ between transverse (to $\widehat{\boldsymbol{B}}$) slices of isoenergy surfaces at energies ε and $\varepsilon + d\varepsilon$. Clearly

$$d^2k_\perp = \frac{d\varepsilon\, d\ell(\varepsilon)}{\big|\partial\varepsilon/\partial \boldsymbol{k}_\perp\big|} \tag{2.84}$$

where $d\ell(\varepsilon)$ is the differential path length in the transverse plane along the surface of energy ε. Note that

$$\left|\frac{\partial\varepsilon}{\partial \boldsymbol{k}_\perp}\right| = \big|\hbar \boldsymbol{v}_\perp\big| = \hbar\,\big|\boldsymbol{v}_\perp \times \widehat{\boldsymbol{B}}\big| = \frac{\hbar^2 c}{eB}\,\big|\dot{\boldsymbol{k}}_\perp\big| \quad . \tag{2.85}$$

[8] In the three-dimensional case, m oscillates but usually does not change sign.

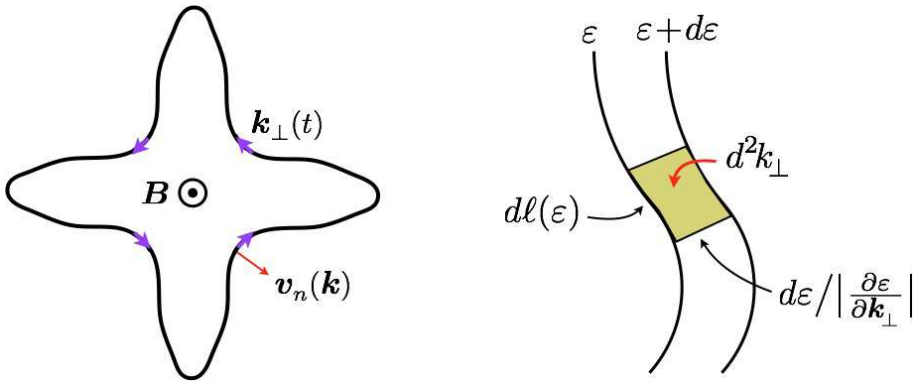

Figure 2.11: Left: Orbit of $\boldsymbol{k}(t)$ in the plane perpendicular to the field $\boldsymbol{B}$. Right: Geometry of Fermi surface orbits in the calculation of the de Haas-van Alphen effect.

Thus, the area enclosed by an orbit of energy ε and parallel wavevector component $k_\parallel = \boldsymbol{k}\cdot\widehat{\boldsymbol{B}}$ is

$$\begin{aligned} A(\varepsilon,k_\parallel) &= \int d^2k_\perp\,\Theta\big(\varepsilon-\varepsilon(\boldsymbol{k}_\perp,k_\parallel)\big) = \int\limits_{-\infty}^{\infty} d\varepsilon'\,\Theta(\varepsilon-\varepsilon')\oint\frac{d\ell(\varepsilon')}{\big|\partial\varepsilon'/\partial\boldsymbol{k}_\perp\big|} \\ &= \frac{eB}{\hbar^2c}\int\limits_{-\infty}^{\infty} d\varepsilon'\,\Theta(\varepsilon-\varepsilon')\oint\frac{d\ell(\varepsilon')}{\big|\dot{\boldsymbol{k}}_\perp\big|} = \frac{eB}{\hbar^2c}\int\limits_{-\infty}^{\varepsilon} d\varepsilon'\,T(\varepsilon',k_\parallel) \quad , \end{aligned} \tag{2.86}$$

where $T(\varepsilon,k_\parallel)$ is the period of the orbit. Note that we have assumed that the surface $\mathcal{S}_\varepsilon$ is closed, *i.e.* that there are no "open orbits" which run periodically across the Brillouin zone. We now have the result

$$\frac{\partial A(\varepsilon,k_\parallel)}{\partial\varepsilon} = \frac{eB}{\hbar^2c}\,T(\varepsilon,k_\parallel) \quad . \tag{2.87}$$

For a free electron in a magnetic field, the orbital period is $2\pi/\omega_{\rm c}$. We accordingly define the *cyclotron mass* by the relation

$$T(\varepsilon,k_\parallel) = \frac{\hbar^2c}{eB}\,\frac{\partial A(\varepsilon,k_\parallel)}{\partial\varepsilon} \equiv \frac{2\pi m_{\rm cyc}c}{eB} \qquad\Longrightarrow\qquad m_{\rm cyc} = \frac{\hbar^2}{2\pi}\,\frac{\partial A(\varepsilon,k_\parallel)}{\partial\varepsilon} \quad . \tag{2.88}$$

Semiclassical quantization then yields the following relation for the energy level spacing:

$$\varepsilon_{n+1}(k_\parallel)-\varepsilon_n(k_\parallel) = \frac{2\pi\hbar}{T\big(\varepsilon_n(k_\parallel),k_\parallel\big)} = \frac{2\pi eB}{\hbar c}\Bigg/\left.\frac{\partial A(\varepsilon,k_\parallel)}{\partial\varepsilon}\right|_{\varepsilon=\varepsilon_n(k_\parallel)} \quad . \tag{2.89}$$

Note that for free electrons,

$$A(\varepsilon,k_\parallel) = \pi\big(\boldsymbol{k}^2-k_\parallel^2\big) = \frac{2\pi m\varepsilon}{\hbar^2} - \pi k_\parallel^2 \quad , \tag{2.90}$$

and so

$$\frac{\partial A(\varepsilon,k_\parallel)}{\partial\varepsilon} = \frac{2\pi m}{\hbar^2} \qquad\Longrightarrow\qquad \varepsilon_{n+1}(k_\parallel)-\varepsilon_n(k_\parallel) = \frac{\hbar eB}{mc} = \hbar\omega_{\rm c} \quad . \tag{2.91}$$

If the semiclassical orbit index n is large, we may approximate $\partial A/\partial\varepsilon$ by a ratio of differences, *viz.*

$$\left.\frac{\partial A(\varepsilon,k_\parallel)}{\partial\varepsilon}\right|_{\varepsilon=\varepsilon_n(k_\parallel)} \simeq \frac{A\big(\varepsilon_{n+1}(k_\parallel),k_\parallel\big)-A\big(\varepsilon_n(k_\parallel),k_\parallel\big)}{\varepsilon_{n+1}(k_\parallel)-\varepsilon_n(k_\parallel)} \quad , \tag{2.92}$$

and invoking Eqn. 2.89 then gives

$$A\big(\varepsilon_{n+1}(k_\parallel),k_\parallel\big)-A\big(\varepsilon_n(k_\parallel),k_\parallel\big)=\frac{2\pi eB}{\hbar c} \quad . \tag{2.93}$$

We then conclude that the areas of the orbits in the plane transverse to $\widehat{\boldsymbol{B}}$ are quantized according to

$$A\big(\varepsilon_n(k_\parallel),k_\parallel\big)=(n+\alpha)\,\frac{2\pi eB}{\hbar c} \quad , \tag{2.94}$$

where α is a constant, a result first derived by Lars Onsager in 1952.

In the free particle model, the each dH-vA oscillation is associated with a Fermi level crossing by one of the Landau levels. Neglecting Zeeman splitting, the semiclassical density of states per unit volume is

$$\begin{aligned} g(\varepsilon) &= \frac{1}{2\pi\ell^2}\sum_n\int\limits_{-\infty}^{\infty}\frac{dk_\parallel}{2\pi}\,\delta\big(\varepsilon-\varepsilon_n(k_\parallel)\big) \\ &= \frac{1}{2\pi\ell^2}\sum_n\int\limits_{-\infty}^{\infty}\frac{dk_\parallel}{2\pi}\,\frac{\delta\big(k_\parallel-\varepsilon_n^{-1}(\varepsilon)\big)}{\big|\partial\varepsilon_n/\partial k_\parallel\big|} \quad , \end{aligned} \tag{2.95}$$

where $\varepsilon_n^{-1}(\varepsilon)=k_\parallel$ when $\varepsilon_n(k_\parallel)=\varepsilon$, *i.e.* it is the inverse function. The DOS is peaked when the denominator vanishes, *i.e.* when $\partial\varepsilon_n/\partial k_\parallel=0$. This entails that the cross sectional Fermi surface area is at a maximum:

$$\frac{\partial}{\partial k_\parallel}A\big(\varepsilon_n(k_\parallel),k_\parallel\big)=\overbrace{\frac{\partial\varepsilon_n(k_\parallel)}{\partial k_\parallel}}^{=0}\cdot\left.\frac{\partial A(\varepsilon,k_\parallel)}{\partial\varepsilon}\right|_{\varepsilon=\varepsilon_n(k_\parallel)}+\left.\frac{\partial A(\varepsilon,k_\parallel)}{\partial k_\parallel}\right|_{\varepsilon=\varepsilon_n(k_\parallel)} \quad . \tag{2.96}$$

Thus, the DOS peaks when the Fermi energy lies on an *extremal orbit*, *i.e.* one which extremizes the cross-sectional Fermi surface area:

$$(n+\alpha)\,\frac{2\pi eB}{\hbar c}=S^*(\varepsilon_{\rm F}) \qquad\Longrightarrow\qquad \Delta\left(\frac{1}{B}\right)=\frac{2\pi e}{\hbar c}\,\frac{1}{S^*(\varepsilon_{\rm F})} \quad , \tag{2.97}$$

where $S^*(\varepsilon)$ is a (possibly multi-valued) function giving the area(s) of the extremal orbits. Since

$$\frac{\hbar\omega_{\rm c}}{k_{\rm B}T}=1.34\times10^{-4}\cdot\frac{B[{\rm T}]}{T[{\rm K}]} \quad , \tag{2.98}$$

(assuming $m=m_{\rm e}$), one needs high fields or low temperatures in order that the oscillations not be washed out by thermal fluctuations.

2.5 Electron Transport in Metals

2.5.1 Drude model

Consider a particle of mass m^* and charge $(-e)$ moving in the presence of an electric field $\boldsymbol{E}$ and magnetic field $\boldsymbol{B}$. Newton's second law says that

$$\frac{d\boldsymbol{p}}{dt} = -e\boldsymbol{E} - \frac{e}{m^*c}\,\boldsymbol{p}\times\boldsymbol{B} - \frac{\boldsymbol{p}}{\tau} \quad , \tag{2.99}$$

where the last term on the RHS is a phenomenological dissipative (*i.e.* frictional) force. The constant τ, which has dimensions of time, is interpreted as the *momentum relaxation time* due to scattering off impurities, lattice excitations (*i.e.* phonons), or sample boundaries. Clearly when $\boldsymbol{E} = \boldsymbol{B} = 0$ we have $\boldsymbol{p}(t) = \boldsymbol{p}(0)\,\exp(-t/\tau)$, which says that $\boldsymbol{p}$ relaxes on a time scale τ.

When $\boldsymbol{E} \neq 0$ but $\boldsymbol{B} = 0$, we have $\dot{\boldsymbol{p}} = -e\boldsymbol{E} - \tau^{-1}\boldsymbol{p}$, and for time-independent $\boldsymbol{E}$ the steady state solution, valid at long times, is $\boldsymbol{p} = -e\tau\boldsymbol{E}$. is then

$$\boldsymbol{j} = -ne\boldsymbol{v} = -ne\,\frac{\boldsymbol{p}}{m^*} = \frac{ne^2\tau}{m^*}\,\boldsymbol{E} \quad . \tag{2.100}$$

Thus there is a linear relationship between the current density $\boldsymbol{j}$ and the applied field $\boldsymbol{E}$. One writes $\boldsymbol{j} = \sigma\boldsymbol{E}$, where σ is the *electrical conductivity*. The above theory says that $\sigma = ne^2\tau/m^*$, where n is the particle density.

We can extend our analysis to include time-dependent fields of the form $\boldsymbol{E}(t) = \mathsf{Re}\left[\,\widehat{\boldsymbol{E}}(\omega)\,e^{-i\omega t}\,\right]$. In steady state, $\boldsymbol{p}$ oscillates with the same frequency, and writing $\boldsymbol{p}(t) = \mathsf{Re}\left[\,\widehat{\boldsymbol{p}}(\omega)\,e^{-i\omega t}\,\right]$, we obtain the relation $(\tau^{-1} - i\omega)\,\widehat{\boldsymbol{p}}(\omega) = -e\widehat{\boldsymbol{E}}(\omega)$, and thus $\boldsymbol{j}(t) = \mathsf{Re}\left[\,\sigma(\omega)\,\widehat{\boldsymbol{E}}(\omega)\,e^{-i\omega t}\,\right]$, with

$$\sigma(\omega) = \frac{ne^2\tau}{m^*}\cdot\frac{1}{1-i\omega\tau} \quad . \tag{2.101}$$

The power density $\boldsymbol{j}(t)\cdot\boldsymbol{E}(t)$ then has terms which are constant, as well as terms oscillating with frequency 2ω. The average power dissipated is obtained by integrating over a period $\Delta t = 2\pi/\omega$, which eliminates the $e^{\pm 2i\omega t}$ terms, resulting in

$$\overline{\boldsymbol{j}(t)\cdot\boldsymbol{E}(t)} = \mathsf{Re}\,\sigma(\omega)\,\big|\widehat{\boldsymbol{E}}(\omega)\big|^2 \quad , \tag{2.102}$$

where the bar denotes time averaging over the period $\Delta t = \pi/\omega$. So it is the real part of the conductivity which is responsible for power dissipation.

Another way to see it: write $\hat{\boldsymbol{j}}(\omega) = \sigma(\omega)\,\widehat{\boldsymbol{E}}(\omega)$, which is a complex vector quantity. If we separate the frequency-dependent conductivity $\sigma(\omega) = \sigma'(\omega) + i\sigma''(\omega)$ into its real and imaginary parts, we see that the $\sigma'(\omega)$ term leads to a current component which is in phase with the drive $\boldsymbol{E}(t)$, while the $\sigma''(\omega)$ term leads to a current component which is 90° out of phase with the drive $\boldsymbol{E}(t)$. The latter current leads to periodic fluctuations in the local energy density, but no net dissipation. The real and imaginary parts of $\sigma(\omega)$ are given by

$$\sigma'(\omega) = \frac{ne^2\tau}{m^*}\cdot\frac{1}{1+\omega^2\tau^2} \qquad , \qquad \sigma''(\omega) = \frac{ne^2\tau}{m^*}\cdot\frac{\omega\tau}{1+\omega^2\tau^2} \quad . \tag{2.103}$$

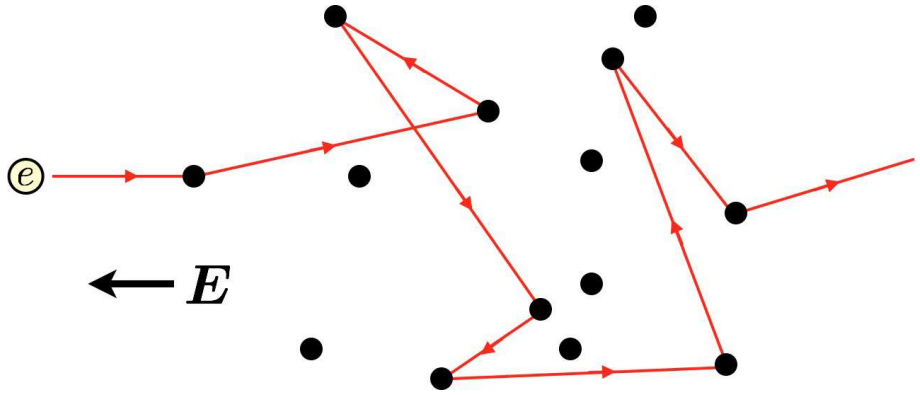

Figure 2.12: Scattering of an electron by impurities in the presence of a uniform electric field $\boldsymbol{E}$ is an example of a biased random walk.

When we try to apply the above physics to electrons in solids, we are confronted with several issues. One obvious question is: what do we mean by n? Filled bands carry no current, because the current density of the $n^{\rm th}$ filled band (accounting for spin),

$$j_n = -2e \int\limits_{\widehat{\Omega}} \frac{d^3k}{(2\pi)^3} \overbrace{\frac{1}{\hbar}\frac{\partial E_n(\boldsymbol{k})}{\partial k^\alpha}}^{v_n(\boldsymbol{k})} = 0 \quad , \tag{2.104}$$

vanishes because $E_n(\boldsymbol{k})$ is periodic in the Brillouin zone, and the integral of the derivative of a periodic function over its period is zero. So the density n must only include contributions from partially filled bands. In fact, the situation is even more complicated because the scattering time can vary from band to band, may be energy-dependent, and there can even be *interband scattering* of electrons. Another question is how we account for scattering within the semiclassical model. We can't just add a term $-\boldsymbol{p}/\tau$ to the right hand side of the equation for $\hbar\dot{\boldsymbol{k}}$, because $\boldsymbol{p} = \hbar\boldsymbol{k}$ is not well-defined in a crystal. A more rigorous approach to transport is based on the Boltzmann equation, which describes how the distribution $f(\boldsymbol{r}, \boldsymbol{k}, t)$ of electron wave packets evolves and takes a steady state form.

The DC conductivity $\sigma = ne^2\tau/m^*$ is proportional to the number of carriers n. Another figure of merit is the *mobility* $\mu = e\tau/m^*$, which is independent of n. Note that the mobility is the ratio of the speed of the electron to the magnitude of the applied field: $\mu = v/E$. The conventional units of mobility are $[\mu] = \mathrm{cm}^2/\mathrm{V}\cdot\mathrm{s}$. Mobility tells us mostly about the scattering time τ. For highly disordered systems, the scattering time τ is short and consequently μ is small. The electrons then move slowly as they execute a biased random walk scattering off impurities in the presence of an electric field (see Fig. 2.12. However, even low mobility systems may have high conductivity, owing to a large density n of conduction electrons. The highest purity semiconductors have mobilities on the order of $10^7\ \mathrm{cm}^2/\mathrm{V}\cdot\mathrm{s}$.

2.5.2 Magnetoresistance and magnetoconductance

Now let's introduce a uniform magnetic field $\boldsymbol{B}$. In component notation, Newton's second law gives

$$\left(\frac{1}{\tau}\,\delta_{\alpha\beta} + \frac{e}{m^*c}\,\varepsilon_{\alpha\beta\gamma}\,B^\gamma\right) p^\beta = -eE^\alpha \quad . \tag{2.105}$$

The current density is $\boldsymbol{j} = -ne\boldsymbol{v} = -ne\boldsymbol{p}/m^*$, hence $\boldsymbol{p} = -m^*\boldsymbol{j}/ne$, and we thus have

$$E^\alpha = \overbrace{\frac{1}{ne^2}\left(\frac{m^*}{\tau}\,\delta_{\alpha\beta} + \frac{e}{c}\,\varepsilon_{\alpha\beta\gamma}\,B^\gamma\right)}^{\rho_{\alpha\beta}} j^\beta \quad . \tag{2.106}$$

The *resistivity matrix* $\rho_{\alpha\beta}(B)$ defines the linear relationship between the electric field $\boldsymbol{E}$ and the current density $\boldsymbol{j}$. At finite frequency, it is easy to see that τ^{-1} must be replaced by $\tau^{-1} - i\omega$, hence, taking $\boldsymbol{B} = B\hat{\boldsymbol{z}}$, the $T = 0$ resistivity tensor is

$$\rho_{\alpha\beta}(\omega, B) = \frac{m^*}{ne^2\tau}\begin{pmatrix} 1 - i\omega\tau & \omega_{\rm c}\tau & 0 \\ -\omega_{\rm c}\tau & 1 - i\omega\tau & 0 \\ 0 & 0 & 1 - i\omega\tau \end{pmatrix} \quad , \tag{2.107}$$

with $\omega_{\rm c} = eB/m^*c$ the cyclotron frequency, as before. Note that the diagonal elements are independent of B, which says that the *magnetoresistance*

$$\Delta\rho_{xx}(B) = \rho_{xx}(B) - \rho_{xx}(0) \tag{2.108}$$

vanishes: $\Delta\rho_{xx}(B) = 0$.

The magnetoconductance, however, does not vanish! Recall that

$$\begin{pmatrix} a & b \\ c & d \end{pmatrix}^{-1} = \frac{1}{ad - bc}\begin{pmatrix} d & -b \\ -c & a \end{pmatrix} \quad , \tag{2.109}$$

from which we have

$$\sigma_{\alpha\beta} = \begin{pmatrix} \sigma_{xx} & \sigma_{xy} & 0 \\ \sigma_{yx} & \sigma_{yy} & 0 \\ 0 & 0 & \sigma_{zz} \end{pmatrix} \quad , \tag{2.110}$$

with

$$\begin{aligned} \sigma_{xx}(\omega, B) = \sigma_{yy}(\omega, B) &= \frac{ne^2\tau}{m^*}\cdot\frac{1 - i\omega\tau}{(1 - i\omega\tau)^2 + (\omega_{\rm c}\tau)^2} \\ \sigma_{yx}(\omega, B) = -\sigma_{xy}(\omega, B) &= \frac{ne^2\tau}{m^*}\cdot\frac{\omega_{\rm c}\tau}{(1 - i\omega\tau)^2 + (\omega_{\rm c}\tau)^2} \\ \sigma_{zz}(\omega, B) &= \frac{ne^2\tau}{m^*}\cdot\frac{1}{1 - i\omega\tau} \quad . \end{aligned} \tag{2.111}$$

Note that σ_{xx} is field-dependent, unlike ρ_{xx}.

Thus far we have assumed that the effective mass tensor $m^*_{\alpha\beta}$ is isotropic. In the general anisotropic case, $m^*_{\alpha\beta}$, which is a symmetric matrix, will have three orthogonal principal axes, which we denote as $\hat{\boldsymbol{x}}$, $\hat{\boldsymbol{y}}$, and $\hat{\boldsymbol{z}}$. In this case, the resistivity tensor assumes the more general form

$$\rho_{\alpha\beta}(\omega, B) = \frac{1}{ne^2} \begin{pmatrix} (\tau^{-1} - i\omega)\, m^*_x & \pm eB_z/c & \mp eB_y/c \\ \mp eB_z/c & (\tau^{-1} - i\omega)\, m^*_y & \pm eB_x/c \\ \pm eB_y/c & \mp eB_x/c & (\tau^{-1} - i\omega)\, m^*_z \end{pmatrix} \quad , \tag{2.112}$$

where (m^*_x, m^*_y, m^*_z) are the three eigenvalues of $m^*_{\alpha\beta}$. The $\pm$ sign in the off-diagonal term distinguishes the case where the Fermi level is just above a quadratic minimum ($+$ sign), versus where it is just below quadratic maximum ($-$ sign). The latter case is described in terms of *holes* in a filled band, as opposed to *electrons* in an empty band. The effective mass tensors are then defined as

$$\big(m^*\big)^{-1}_{\alpha\beta} = \pm \frac{1}{\hbar^2} \frac{\partial^2 E_n(\boldsymbol{k})}{\partial k^\alpha\, \partial k^\beta} \quad , \tag{2.113}$$

where the top sign corresponds to electrons and the bottom sign to holes.

Note that the diagonal elements in Eqn. 2.112 are still independent of B and there is no magnetoresistance. Taking $\boldsymbol{B}$ along $\hat{\boldsymbol{z}}$, the corresponding elements of $\sigma_{\alpha\beta}$ are

$$\begin{aligned} \sigma_{xx}(\omega, B) &= \frac{ne^2\tau}{m^*_x} \cdot \frac{1 - i\omega\tau}{(1 - i\omega\tau)^2 + (\omega_{\rm c}\tau)^2} \\ \sigma_{yy}(\omega, B) &= \frac{ne^2\tau}{m^*_y} \cdot \frac{1 - i\omega\tau}{(1 - i\omega\tau)^2 + (\omega_{\rm c}\tau)^2} \\ \sigma_{yx}(\omega, B) &= \pm \frac{ne^2\tau}{m^*_\perp} \cdot \frac{\omega_{\rm c}\tau}{(1 - i\omega\tau)^2 + (\omega_{\rm c}\tau)^2} \\ \sigma_{zz}(\omega, B) &= \frac{ne^2\tau}{m^*_z} \cdot \frac{1}{1 - i\omega\tau} \quad , \end{aligned} \tag{2.114}$$

where $\omega_{\rm c} = eB/m^*_\perp c$ and $m^*_\perp = \sqrt{m^*_x m^*_y}$.

2.5.3 Hall effect in high fields

In the high field limit, we have that the resistivity and conductivity tensors are purely off-diagonal, with

$$\rho_{xy}(B) = \pm \frac{B}{nec} \qquad , \qquad \sigma_{xy}(B) = \mp \frac{nec}{B} \tag{2.115}$$

where the upper sign is again for conduction electrons, and the bottom sign for valence holes. Thus, the high field Hall effect may be used to determine the carrier concentration:

$$n = \pm \lim_{B\to\infty} \frac{B}{ec\rho_{xy}(B)} \quad . \tag{2.116}$$

2.5.4 Cyclotron resonance in semiconductors

A typical value for the effective mass in semiconductors is $m^* \sim 0.1\, m_{\rm e}$. From

$$\frac{e}{m_{\rm e}\, c} = 1.75 \times 10^7 \,{\rm Hz/G}\,, \tag{2.117}$$

we find that $eB/m^*c = 1.75 \times 10^{11}$ Hz in a field of $B = 1\,$kG. In metals, the disorder is such that even at low temperatures $\omega_{\rm c}\tau$ typically is small. In semiconductors, however, the smallness of m^* and the relatively high purity (sometimes spectacularly so) mean that $\omega_{\rm c}\tau$ can get as large as 10^3 at modest fields. This allows for a measurement of the effective mass tensor using the technique of *cyclotron resonance*.

The absorption of electromagnetic radiation is proportional to the dissipative (*i.e.* real) part of the diagonal elements of $\sigma_{\alpha\beta}(\omega, B)$, which, again taking $\boldsymbol{B}$ along $\hat{\boldsymbol{z}}$, is given by

$$\sigma'_{xx}(\omega, B) = \frac{ne^2\tau}{m^*_x}\,\frac{1 + (\lambda^2+1)s^2}{1 + 2(\lambda^2+1)s^2 + (\lambda^2-1)^2 s^4}\,, \tag{2.118}$$

where $\lambda = B/B_\omega$, with $B_\omega = m^*_\perp c\omega/e$, and $s = \omega\tau$. For fixed ω, the conductivity $\sigma'_{xx}(B)$ is then peaked at $B = B^*$. When $\omega\tau \gg 1$ and $\omega_{\rm c}\tau \gg 1$, B^* approaches B_ω, where $\sigma'_{xx}(\omega, B_\omega) = ne^2\tau/2m^*_x$. By measuring B_ω one can extract the quantity $m^*_\perp = eB_\omega/\omega c$. Varying the direction of the magnetic field, the entire effective mass tensor may be determined.

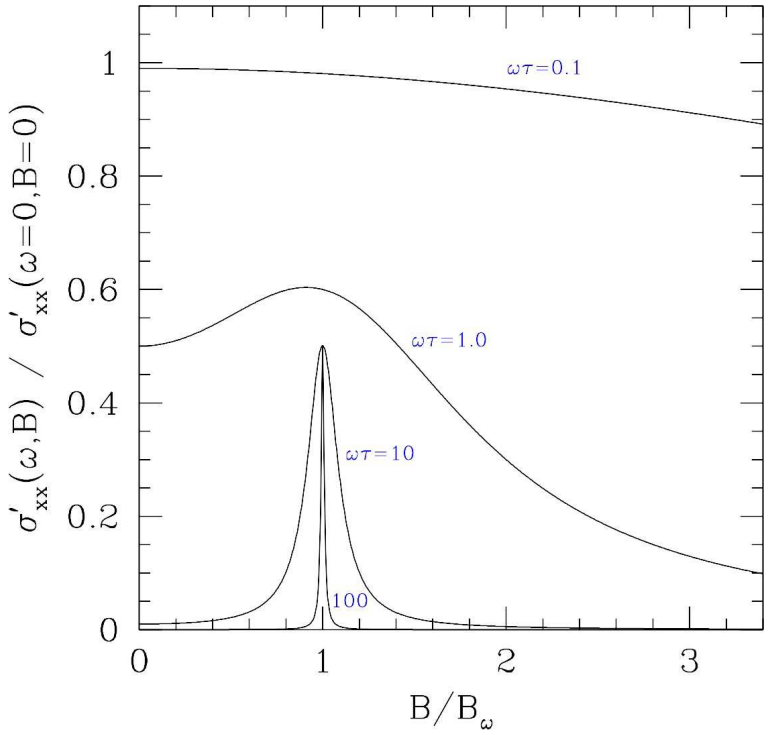

Figure 2.13: Theoretical cyclotron resonance peaks as a function of B/B_ω for different values of $\omega\tau$.

For finite $\omega\tau$, we can differentiate the above expression to obtain the location of the cyclotron resonance peak. One finds $B = (1+\alpha)^{1/2}\, B_\omega$, with

$$\begin{aligned}\alpha &= \frac{-(2s^2+1) + \sqrt{(2s^2+1)^2 - 1}}{s^2} \\ &= -\frac{1}{4s^4} + \frac{1}{8s^6} + \mathcal{O}(s^{-8})\ .\end{aligned}$$

As depicted in fig. 2.13, the resonance peak shifts to the left of B_ω for finite values of $\omega\tau$. The peak collapses to $B = 0$ when $\omega\tau \le 1/\sqrt{3} = 0.577$.

2.5.5 Magnetoresistance in a two band model

For a semiconductor with both electrons and holes present – a situation not uncommon to metals either (*e.g.* Aluminum) – each band contributes to the conductivity. The individual band conductivities are *additive* because the electron and hole conduction processes occur *in parallel*, *i.e.*

$$\sigma_{\alpha\beta}(\omega) = \sum_n \sigma^{(n)}_{\alpha\beta}(\omega)\ , \tag{2.119}$$

where $\sigma^{(n)}_{\alpha\beta}$ is the conductivity tensor for band n, which may be computed in either the electron or hole picture (whichever is more convenient). We assume here that the two bands c and v may be treated independently, *i.e.* there is no interband scattering to account for.

The resistivity tensor of each band, $\rho^{(n)}_{\alpha\beta}$ exhibits no magnetoresistance, as we have found. However, if two bands are present, the total resistivity tensor ρ is obtained from $\rho^{-1} = \rho_{\mathrm{c}}^{-1} + \rho_{\mathrm{v}}^{-1}$, and

$$\rho = \left(\rho_{\mathrm{c}}^{-1} + \rho_{\mathrm{v}}^{-1}\right)^{-1} \tag{2.120}$$

will in general exhibit the phenomenon of magnetoresistance.

Explicitly, then, let us consider a model with isotropic and nondegenerate conduction band minimum and valence band maximum. Taking $\boldsymbol{B} = B\hat{\boldsymbol{z}}$, we have

$$\begin{aligned}\rho_{\mathrm{c}} &= \frac{(1-i\omega\tau_{\mathrm{c}})m_{\mathrm{c}}}{n_{\mathrm{c}}e^2\tau_{\mathrm{c}}}\,\mathbb{I} + \frac{B}{n_{\mathrm{c}}ec}\begin{pmatrix}0&1&0\\-1&0&0\\0&0&0\end{pmatrix} = \begin{pmatrix}\alpha_{\mathrm{c}}&\beta_{\mathrm{c}}&0\\-\beta_{\mathrm{c}}&\alpha_{\mathrm{c}}&0\\0&0&\alpha_{\mathrm{c}}\end{pmatrix} \\ \rho_{\mathrm{v}} &= \frac{(1-i\omega\tau_{\mathrm{v}})m_{\mathrm{v}}}{n_{\mathrm{v}}e^2\tau_{\mathrm{v}}}\,\mathbb{I} - \frac{B}{n_{\mathrm{v}}ec}\begin{pmatrix}0&1&0\\-1&0&0\\0&0&0\end{pmatrix} = \begin{pmatrix}\alpha_{\mathrm{v}}&-\beta_{\mathrm{v}}&0\\\beta_{\mathrm{v}}&\alpha_{\mathrm{v}}&0\\0&0&\alpha_{\mathrm{v}}\end{pmatrix}\quad ,\end{aligned} \tag{2.121}$$

where

$$\begin{aligned}\alpha_{\mathrm{c}} &= \frac{(1-i\omega\tau_{\mathrm{c}})m_{\mathrm{c}}}{n_{\mathrm{c}}e^2\tau_{\mathrm{c}}} \qquad & \beta_{\mathrm{c}} &= \frac{B}{n_{\mathrm{c}}ec} \\ \alpha_{\mathrm{v}} &= \frac{(1-i\omega\tau_{\mathrm{v}})m_{\mathrm{v}}}{n_{\mathrm{v}}e^2\tau_{\mathrm{v}}} \qquad & \beta_{\mathrm{v}} &= \frac{B}{n_{\mathrm{v}}ec}\quad ,\end{aligned} \tag{2.122}$$

we obtain for the upper left 2×2 block of ρ:

$$\rho_\perp = \left[\left(\frac{\alpha_{\rm v}}{\alpha_{\rm v}^2+\beta_{\rm v}^2} + \frac{\alpha_{\rm c}}{\alpha_{\rm c}^2+\beta_{\rm c}^2} \right)^2 + \left(\frac{\beta_{\rm v}}{\alpha_{\rm v}^2+\beta_{\rm v}^2} + \frac{\beta_{\rm c}}{\alpha_{\rm c}^2+\beta_{\rm c}^2} \right)^2 \right]^{-1} \times \begin{pmatrix} \frac{\alpha_{\rm v}}{\alpha_{\rm v}^2+\beta_{\rm v}^2} + \frac{\alpha_{\rm c}}{\alpha_{\rm c}^2+\beta_{\rm c}^2} & \frac{\beta_{\rm v}}{\alpha_{\rm v}^2+\beta_{\rm v}^2} + \frac{\beta_{\rm c}}{\alpha_{\rm c}^2+\beta_{\rm c}^2} \\ -\frac{\beta_{\rm v}}{\alpha_{\rm v}^2+\beta_{\rm v}^2} - \frac{\beta_{\rm c}}{\alpha_{\rm c}^2+\beta_{\rm c}^2} & \frac{\alpha_{\rm v}}{\alpha_{\rm v}^2+\beta_{\rm v}^2} + \frac{\alpha_{\rm c}}{\alpha_{\rm c}^2+\beta_{\rm c}^2} \end{pmatrix} \quad , \tag{2.123}$$

from which we compute the magnetoresistance,

$$\frac{\rho_{xx}(B)-\rho_{xx}(0)}{\rho_{xx}(0)} = \frac{\gamma_{\rm c}\,\gamma_{\rm v}\left(\frac{\gamma_{\rm c}}{n_{\rm c}ec} - \frac{\gamma_{\rm v}}{n_{\rm v}ec}\right)^2 B^2}{(\gamma_{\rm c}+\gamma_{\rm v})^2 + (\gamma_{\rm c}\,\gamma_{\rm v})^2\left(\frac{1}{n_{\rm c}ec} + \frac{1}{n_{\rm v}ec}\right)^2 B^2} \quad , \tag{2.124}$$

where

$$\gamma_{\rm c} \equiv \alpha_{\rm c}^{-1} = \frac{n_{\rm c}e^2\tau_{\rm c}}{m_{\rm c}} \cdot \frac{1}{1-i\omega\tau_{\rm c}}$$

$$\gamma_{\rm v} \equiv \alpha_{\rm v}^{-1} = \frac{n_{\rm v}e^2\tau_{\rm v}}{m_{\rm v}} \cdot \frac{1}{1-i\omega\tau_{\rm v}} \quad .$$

Note that the magnetoresistance is *positive* within the two band model, and that it *saturates* in the high field limit:

$$\frac{\rho_{xx}(B\to\infty)-\rho_{xx}(0)}{\rho_{xx}(0)} = \frac{\gamma_{\rm c}\,\gamma_{\rm v}\left(\frac{\gamma_{\rm c}}{n_{\rm c}ec} - \frac{\gamma_{\rm v}}{n_{\rm v}ec}\right)^2}{(\gamma_{\rm c}\,\gamma_{\rm v})^2\left(\frac{1}{n_{\rm c}ec} + \frac{1}{n_{\rm v}ec}\right)^2} \quad . \tag{2.125}$$

The longitudinal resistivity is found to be

$$\rho_{zz} = (\gamma_{\rm c}+\gamma_{\rm v})^{-1} \quad , \tag{2.126}$$

and is independent of B.

In an intrinsic semiconductor, $n_{\rm c} = n_{\rm v} \propto \exp(-E_{\rm g}/2k_{\rm B}T)$, and $\Delta\rho_{xx}(B)/\rho_{xx}(0)$ is finite even as $T \to 0$. In the extrinsic (*i.e.* doped) case, one of the densities (say, $n_{\rm c}$ in a p-type material) vanishes much more rapidly than the other, and the magnetoresistance vanishes with the ratio $n_{\rm c}/n_{\rm v}$.

2.5.6 Optical reflectivity of metals and semiconductors

What happens when an electromagnetic wave is incident on a metal? Inside the metal we have Maxwell's equations:

$$\boldsymbol{\nabla}\times\boldsymbol{H} = \frac{4\pi}{c}\,\boldsymbol{j} + \frac{1}{c}\frac{\partial \boldsymbol{D}}{\partial t} \qquad \Longrightarrow \qquad i\boldsymbol{k}\times\boldsymbol{B} = \left(\frac{4\pi\sigma}{c} - \frac{i\omega}{c}\right)\boldsymbol{E} \tag{2.127}$$

and

$$\boldsymbol{\nabla}\times\boldsymbol{E} = -\frac{1}{c}\frac{\partial \boldsymbol{B}}{\partial t} \qquad \Longrightarrow \qquad i\boldsymbol{k}\times\boldsymbol{E} = \frac{i\omega}{c}\boldsymbol{B} \tag{2.128}$$

and

$$\boldsymbol{\nabla}\cdot\boldsymbol{E} = \boldsymbol{\nabla}\cdot\boldsymbol{B} = 0 \qquad \Longrightarrow \qquad i\boldsymbol{k}\cdot\boldsymbol{E} = i\boldsymbol{k}\cdot\boldsymbol{B} = 0 \quad , \tag{2.129}$$

where we've assumed $\mu = \epsilon = 1$ inside the metal, ignoring polarization due to virtual interband transitions (*i.e.* from core electrons). Hence,

$$\begin{aligned} \boldsymbol{k}^2 &= \frac{\omega^2}{c^2} + \frac{4\pi i\omega}{c^2}\,\sigma(\omega) \\ &= \frac{\omega^2}{c^2} + \frac{\omega_{\rm p}^2}{c^2}\,\frac{i\omega\tau}{1-i\omega\tau} \equiv \epsilon(\omega)\,\frac{\omega^2}{c^2} \quad , \end{aligned} \tag{2.130}$$

where $\omega_{\rm p} = \sqrt{4\pi n e^2/m^*}$ is the *plasma frequency* for the conduction band. The dielectric function,

$$\epsilon(\omega) = 1 + \frac{4\pi i\sigma(\omega)}{\omega} = 1 + \frac{\omega_{\rm p}^2}{\omega^2}\,\frac{i\omega\tau}{1-i\omega\tau} \tag{2.131}$$

determines the complex refractive index, $N(\omega) = \sqrt{\epsilon(\omega)}$, leading to the electromagnetic dispersion relation $k = N(\omega)\,\omega/c$.

Consider a wave normally incident upon a metallic surface normal to $\hat{\boldsymbol{z}}$. In the vacuum ($z < 0$), we write

$$\begin{aligned} \boldsymbol{E}(\boldsymbol{r},t) &= E_1\,\hat{\boldsymbol{x}}\,e^{i\omega z/c}e^{-i\omega t} + E_2\,\hat{\boldsymbol{x}}\,e^{-i\omega z/c}e^{-i\omega t} \\ \boldsymbol{B}(\boldsymbol{r},t) &= \frac{c}{i\omega}\,\boldsymbol{\nabla}\times\boldsymbol{E} = E_1\,\hat{\boldsymbol{y}}\,e^{i\omega z/c}e^{-i\omega t} - E_2\,\hat{\boldsymbol{y}}\,e^{-i\omega z/c}e^{-i\omega t} \end{aligned} \tag{2.132}$$

while in the metal ($z > 0$),

$$\begin{aligned} \boldsymbol{E}(\boldsymbol{r},t) &= E_3\,\hat{\boldsymbol{x}}\,e^{iN\omega z/c}e^{-i\omega t} \\ \boldsymbol{B}(\boldsymbol{r},t) &= \frac{c}{i\omega}\,\boldsymbol{\nabla}\times\boldsymbol{E} = NE_3\,\hat{\boldsymbol{y}}\,e^{iN\omega z/c}e^{-i\omega t} \quad . \end{aligned} \tag{2.133}$$

Continuity of $\boldsymbol{E}\times\hat{\boldsymbol{n}}$ gives $E_1 + E_2 = E_3$. Continuity of $\boldsymbol{H}\times\hat{\boldsymbol{n}}$ gives $E_1 - E_2 = NE_3$. Thus,

$$\frac{E_2}{E_1} = \frac{1-N}{1+N} \qquad , \qquad \frac{E_3}{E_1} = \frac{2}{1+N} \tag{2.134}$$

and the reflection and transmission coefficients are

$$\begin{aligned} R(\omega) &= \left|\frac{E_2}{E_1}\right|^2 = \left|\frac{1-N(\omega)}{1+N(\omega)}\right|^2 \\ T(\omega) &= \left|\frac{E_3}{E_1}\right|^2 = \frac{4}{\left|1+N(\omega)\right|^2} \quad . \end{aligned} \tag{2.135}$$

We've now solved the electromagnetic boundary value problem.

Typical values – For a metal with $n = 10^{22}\,{\rm cm}^3$ and $m^* = m_{\rm e}$, the plasma frequency is $\omega_{\rm p} = 5.7\times10^{15}\,{\rm s}^{-1}$. The scattering time varies considerably as a function of temperature. In high purity copper at $T = 4\,{\rm K}$, $\tau \approx 2\times10^{-9}\,{\rm s}$ and $\omega_{\rm p}\tau \approx 10^7$. At $T = 300\,{\rm K}$, $\tau \approx 2\times10^{-14}\,{\rm s}$ and $\omega_{\rm p}\tau \approx 100$. In either case, $\omega_{\rm p}\tau \gg 1$. There are then three regimes to consider:

Low frequencies : $\omega\tau \ll 1 \ll \omega_{\rm p}\tau$

We may approximate $1 - i\omega\tau \approx 1$, hence

$$\begin{aligned} N^2(\omega) &= 1 + \frac{i\,\omega_{\rm p}^2\tau}{\omega(1-i\omega\tau)} \approx \frac{i\,\omega_{\rm p}^2\tau}{\omega} \\ N(\omega) &\approx \frac{1+i}{\sqrt{2}}\left(\frac{\omega_{\rm p}^2\tau}{\omega}\right)^{1/2} \quad\Longrightarrow\quad R \approx 1 - \frac{2\sqrt{2\omega\tau}}{\omega_{\rm p}\tau} \quad . \end{aligned} \tag{2.136}$$

Hence $R \approx 1$ and the metal reflects.

Intermediate frequencies : $1 \ll \omega\tau \ll \omega_{\rm p}\tau$

In this regime,

$$N^2(\omega) \approx 1 - \frac{\omega_{\rm p}^2}{\omega^2} + \frac{i\,\omega_{\rm p}^2}{\omega^3\tau} \tag{2.137}$$

which is almost purely real and negative. Hence N is almost purely imaginary and $R \approx 1$. (To lowest nontrivial order, $R = 1 - 2/\omega_{\rm p}\tau$.) Still high reflectivity.

High frequencies : $1 \ll \omega_{\rm p}\tau \ll \omega\tau$

Here we have

$$N^2(\omega) \approx 1 - \frac{\omega_{\rm p}^2}{\omega^2} \quad\Longrightarrow\quad R = \frac{\omega_{\rm p}}{2\omega} \tag{2.138}$$

and $R \ll 1$ – the metal is transparent at frequencies large compared to $\omega_{\rm p}$.

2.5.7 Optical conductivity of semiconductors

In our analysis of the electrodynamics of metals, we assumed that the dielectric constant due to all the filled bands was simply $\epsilon = 1$. This is not quite right. We should instead have written

$$\begin{aligned} \boldsymbol{k}^2 &= \epsilon_\infty\,\frac{\omega^2}{c^2} + \frac{4\pi i\omega\sigma(\omega)}{c^2} \\ \epsilon(\omega) &= \epsilon_\infty\left\{1 + \frac{\omega_{\rm p}^2}{\omega^2}\frac{i\omega\tau}{1-i\omega\tau}\right\} \ , \end{aligned} \tag{2.139}$$

where ϵ_∞ is the dielectric constant due to virtual transitions to fully occupied (*i.e.* core) and fully unoccupied bands, at a frequency small compared to the interband frequency. The plasma frequency is now defined as

$$\omega_{\rm p} = \left(\frac{4\pi n e^2}{m^*\,\epsilon_\infty}\right)^{1/2} \tag{2.140}$$

where n is the conduction electron density. Note that $\epsilon(\omega \to \infty) = \epsilon_\infty$, although again this is only true for ω smaller than the gap to neighboring bands. It turns out that for insulators one can write

$$\epsilon_\infty \simeq 1 + \frac{\omega_{\rm pv}^2}{\omega_{\rm g}^2} \tag{2.141}$$

where $\omega_{\rm pv} = \sqrt{4\pi n_{\rm v} e^2/m_{\rm e}}$, with $n_{\rm v}$ the number density of valence electrons, and $\omega_{\rm g}$ is the energy gap between valence and conduction bands. In semiconductors such as Si and Ge, $\omega_{\rm g} \sim 4\,{\rm eV}$, while $\omega_{\rm pv} \sim 16\,{\rm eV}$, hence $\epsilon_\infty \sim 17$, which is in rough agreement with the experimental values of ~ 12 for Si and ~ 16 for Ge. In metals, the band gaps generally are considerably larger.

There are some important differences to consider in comparing semiconductors and metals:

- The carrier density n typically is much smaller in semiconductors than in metals, ranging from $n \sim 10^{16}\,{\rm cm}^{-3}$ in intrinsic (*i.e.* undoped, thermally excited at room temperature) materials to $n \sim 10^{19}\,{\rm cm}^{-3}$ in doped materials.
- $\epsilon_\infty \approx 10 - 20$ and $m^*/m_{\rm e} \approx 0.1$. The product $\epsilon_\infty m^*$ thus differs only slightly from its free electron value.

Since $n_{\rm semi} \lesssim 10^{-4}\, n_{\rm metal}$, one has

$$\omega_{\rm p}^{\rm semi} \approx 10^{-2}\, \omega_{\rm p}^{\rm metal} \approx 10^{-14}\,{\rm s}\,. \tag{2.142}$$

In high purity semiconductors the mobility $\mu = e\tau/m^* \gtrsim 10^5\,{\rm cm}^2/{\rm vs}$ the low temperature scattering time is typically $\tau \approx 10^{-11}\,{\rm s}$. Thus, for $\omega \gtrsim 3 \times 10^{15}\,{\rm s}^{-1}$ in the optical range, we have $\omega\tau \gg \omega_{\rm p}\tau \gg 1$, in which case $N(\omega) \approx \sqrt{\epsilon_\infty}$ and the reflectivity is

$$R = \left| \frac{1 - \sqrt{\epsilon_\infty}}{1 + \sqrt{\epsilon_\infty}} \right|^2 . \tag{2.143}$$

Taking $\epsilon_\infty = 10$, one obtains $R = 0.27$, which is high enough so that polished Si wafers appear shiny.